Technische Universiteit
Eindhoven
University of Technology

Department of Mechanical Engineering
Automotive Technology Master Program

Modeling and Identification of Urban Bus Dynamics

Internship Report - DC 2017.053.

Amin Sehati 0980662

Supervisor:
ir. B. (Boulaid) Boulkroune (Flanders Make)
Prof.dr. H. (Henk) Nijmeijer (TU/e)

An Assignment at Flanders Make, Lommel, Belgium

Eindhoven, September 2016

Abstract

Autonomous vehicles are the result of growing interest in safe, intelligent and convenient transportation. Over the last years, many automotive manufacturers have shown their investments on developing autonomous commercial vehicles. Hence, controllers are needed for dealing with such systems. In order to design these controllers, understanding the dynamics of the vehicle is a must. This internship is focused on modeling and identification of the dynamics of an urban bus. As the first step, different vehicle models are investigated; one of which has been chosen to provide the required accuracy to give the states of the vehicle. Furthermore, the model has been extended and adapted for the dynamics of the bus by adding roll and pitch motions to the equations of motion. Dugoff tire model has been selected to obtain the tire lateral forces. Also for identification purposes, it was necessary to simplify the model to only longitudinal, lateral, roll or pitch motion. After modeling, identification methods are used to find the unknown model parameters. Hence, some tests were done with the vehicle in order to acquire the required identification data. After obtaining the parameter values, the model output has been validated using experimental data. The validation shows that the model can simulate the dynamic responses of the test vehicle by an acceptable accuracy. However, due to lack of equipment to measure the model inputs, the inputs were estimated in order to simulate the same input signals as in the experiments.

Preface

This report has been written under the supervision of prof.dr. Henk Nijmeijer from Eindhoven University of Technology and ir. Boulaid Boulkroune from Flanders Make. It serves as documentation of my research during the internship, which has been made from August 2016 until December 2016. It presents the results of a study towards modeling and identification of an urban bus dynamics.

We sincerely express our gratitude to our supervisors for their advice, guidance and support throughout the internship. Furthermore, I would like to thank the following persons in particular for all the help they provided: First of all dr. Norddin El Ghouti, for providing the opportunity to work at Flanders Make. I would like to thank Sebastiaan van Aalst for all his technical help during the internship and the guidance he provided. Next I would like to thank Koen Sannen for the opportunity to implement the experiments on the testing vehicle. I would also like to thank Flanders Make, for providing us with the necessary tools, vehicle and testing environment. It was a pleasure to be able to work on this internship. Finally, we would also like to thank everyone else who helped and supported us, but is not mentioned here.

Lommel, December, 2016
Amin Sehati

Contents

Nomenclature

α	Lateral slip
δ	Steering angle
κ	Longitudinal slip
θ	Pitch angle
φ	Roll angle
a_x	Longitudinal acceleration
a_y	Lateral acceleration
C_θ	Pitch damping
C_{φ_1}, C_{φ_2}	Front and rear roll damping
F_x, F_y, F_z	Tire force
g	Gravitational acceleration
h'	Roll center height
h''	Pitch center height
H_r	Roof height
h_{CG}	Center of gravity height
i_F	Final drive ratio
i_G	Gear ratio
I_w	Wheel moment of inertia
I_{xx}, I_{yy}, I_{zz}	Moment of inertia
K_θ	Pitch stiffness
K_{φ_1}, K_{φ_2}	Front and rear roll stiffness
l	Wheelbase
l_f	Center of gravity distance from front axle
l_r	Center of gravity distance from rear axle
m	Vehicle mass
M_b	Brake moment

Q_r	Yaw moment
Q_u	Longitudinal forces
Q_v	Lateral forces
r	Yaw rate
r_w	Wheel radius
T	Kinetic energy
T_e	Engine torque
t_f	Front track width
t_r	Rear track width
T_w	Wheel torque
U	Potential energy
v_x	Longitudinal velocity
v_y	Lateral velocity

Chapter 1

Introduction

1.1 Context

In the framework of Environmental Modeling for Automated Driving and Active Safety (EMDAS) project, an urban bus automation is studied with and for Flemish companies to prepare for an expected potential market within the next 5 years. The project partners were Siemens, TomTom, Transport Mobility Leuven, University Gent, VDL Bus Coach and Xenics Infrared Solutions. Autonomously guiding of such a vehicle requires controllers. Hence, understanding the bus dynamics is necessary to design the controllers. However, design and implementation of the controllers are out of the scope of this internship and has to be done as a future work in the company. The goal is to provide a model of the bus dynamics which describes its dominant motions. Since bus dynamics can be more complex than passenger car due to its rather huge mass and inertia, the model needs to capture influential motions such as roll and pitch. This model is going to be implemented in simulation software that can simulate different environment and scenarios and can be used to test the controller that will be later added to the model. Five models have been developed: a 5 degree of freedom vehicle model which can be used in complex response analysis such as emergency-lane-change maneuver (full-state model), a simple longitudinal model which will be used to control the longitudinal motion, a lateral model which will be used to identify the lateral tire parameters, and roll and pitch models to identify the vehicle roll and pitch parameters, respectively.

1.2 Literature survey

To analyse the dynamic behavior of vehicles, different models are used for one of the four purposes: vertical dynamics simulation, handling behavior simulation, rotational dynamics simulation or full dynamics simulation. Since vertical dynamics simulation is mostly used to study comfort and tyre compression of the vehicle which is not the purpose of this study, it will be no longer discussed in this report. The other three purposes are presented in the following sections.

1.2.1 Handling behaviour simulation

When handling behaviour is investigated, longitudinal, lateral and yaw dynamics of the vehicle should be considered in a planar motion. The most common handling model is the single track vehicle model (bicycle model) [2]. In this model, the left and right tires are lumped into a single equivalent tire for the front and rear axle. Due to the simplicity of this model, it can be used for identification purposes and real-time implementations [4].

1.2.2 Rotational dynamics simulation

Rotational dynamic models are mostly known as roll motion model and pitch motion model. They can be used to identify the roll and pitch motion parameters or can be added to handling simulations in order to study the roll or pitch motions [12]. The roll motion can be modeled by two torsion springs and two torsion dampers, one at each end of the axis and representing front and rear vehicles suspension, which generate torques opposed to the roll [5]. By applying the same theory used for the roll motion, pitch motion of the vehicle can be studied as well. Hence, pitch axis is defined by a torsion spring and damper reacting to the longitudinal acceleration in this case [5].

1.2.3 Full dynamics simulation

Full dynamics simulation, also known as full-state vehicle simulation is a tool to analyze the overall dynamics of the vehicle in different situations (e.g. obstacle avoidance or emergency braking). The model used for this simulation is mostly the combination of other models. It can be a combination of four vertical models (movement of the four unsprung masses, the vertical movement of the sprung mass and the roll and pitch angle of the sprung mass) [15] or two single track model in parallel together with roll and pitch motion model which in this study is called double-track vehicle model [5]. A similar model but with the roll dynamics excluded, can be found in [10].

1.3 Research question

Modeling and identification of a vehicle is not a neural practice. However, modeling an urban bus which can show different dynamic behaviours than passenger vehicles due to its huge mass and inertia, can be more complex. Since there was no access to the CAN data and the fact that many tests may not be feasible to be implemented due to the size and mass of such a vehicle, identification of urban bus can be more challenging than passenger cars. Hence, the question is that whether it is possible to model and identify urban bus dynamics with current methods and still achieve an acceptable accuracy in Simulation outputs which are the vehicle states.

1.4 Report outline

In Chapter 2, modeling of the vehicle is explained. The first and second parts show the handling behaviour and rotational models that have been used for identification purposes. The third part presents the full-state vehicle model developed to analyze dynamics of the vehicle in critical situations (e.g. obstacle avoidance). The constant parameters of the models are identified in two separate chapters. In Chapter 3, all parameter values, that can be identified without experiments, are discussed. In Chapter 4, the experiments performed on the test vehicle are explained together with the obtained result. The validation process is explained in Chapter 5. In this chapter, one of the performed test maneuvers has been selected to validate the double-track vehicle model (full-state). Lastly, the possible future work that can improve the accuracy and validity of the models is described in Chapter 6.

Chapter 2

Modeling

One of the main goals of the internship was to model the test vehicle in order to analyze the vehicle dynamic responses in different maneuvers such as obstacle avoidance. Hence a 5-DOF model is developed as the vehicle dynamics model for handling studies. However, it is difficult to identify the unknown model parameters by using the 5-DOF vehicle model. Hence, the model has been split for identification purposes. Furthermore, a simple longitudinal model was believed to be sufficient to be implemented on the company's longitudinal controller. So another model has been developed for that purpose.
The first part of this chapter describes the 5-DOF vehicle model. The model developed for the company's longitudinal controller is explained in the second part, which is followed by the third and fourth parts which are the models developed for identification purposes. The remaining parts describe the models that have to be added to complete the 5-DOF vehicle model in Simulink.

2.1 Vehicle dynamics model for handling studies

A 5-DOF vehicle model has been developed for this study. This model is capable of modeling the dynamics response of a vehicle in longitudinal, lateral and transverse directions in order to be used for simulation purposes. In other words, except the motion in X and Y direction (2-DOF), this model can also simulate the vehicle behaviour in Yaw, Pitch and Roll motion (3-DOF). It should be mentioned that the vertical displacement of the vehicle is not relevant for this study.

2.1.1 Equations of motion for 5-DOF vehicle model

The aim of this chapter is to derive the differential equations for the five degree of freedom vehicle model as can be seen in Figure 2.1. As for the sign convention, it should be mentioned that ISO axis system has been used in this chapter.

Lagrange's equations have been employed to derive the equations of motion. In general, n generalized coordinates q_i are selected to describe a system with n degrees of freedom. The relation between kinetic energy T, potential energy U and external generalized forces Q_i can be seen in the following equation which shows the Lagrange equation for coordinate q_i.

$$\frac{d}{dt}\frac{\partial T}{\partial \dot{q}_i} - \frac{\partial T}{\partial q_i} + \frac{\partial U}{\partial q_i} = Q_i \tag{2.1}$$

In order to convert the Cartesian coordinates X, Y and Ψ velocities to body-fixed frame velocities

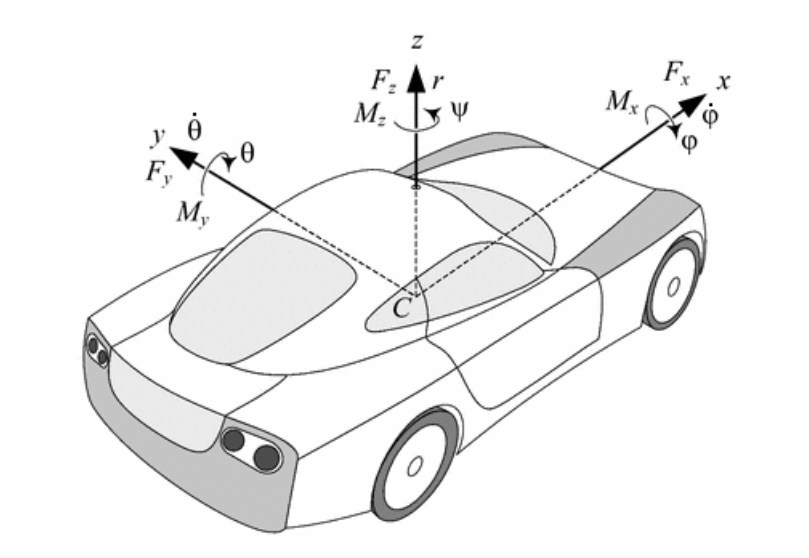

Figure 2.1: Vehicle motion

v_x, v_y and r, following relations have been used as they can be derived from Figure 2.2.

$$\begin{cases} v_x = \dot{X}\cos\Psi + \dot{Y}\sin\Psi \\ v_y = -\dot{X}\sin\Psi + \dot{Y}\cos\Psi \\ r = \dot{\Psi} \end{cases} \tag{2.2}$$

Also the kinetic energy can be expressed in terms of body-fixed frame velocities.

$$\begin{aligned} \frac{\partial T}{\partial \dot{X}} &= \frac{\partial T}{\partial v_x}\frac{\partial v_x}{\partial \dot{X}} + \frac{\partial T}{\partial v_y}\frac{\partial v_y}{\partial \dot{X}} = \frac{\partial T}{\partial v_x}\cos\Psi - \frac{\partial T}{\partial v_y}\sin\Psi \\ \frac{\partial T}{\partial \dot{Y}} &= \frac{\partial T}{\partial v_x}\frac{\partial v_x}{\partial \dot{Y}} + \frac{\partial T}{\partial v_y}\frac{\partial v_y}{\partial \dot{Y}} = \frac{\partial T}{\partial v_x}\sin\Psi - \frac{\partial T}{\partial v_y}\cos\Psi \\ \frac{\partial T}{\partial \dot{\Psi}} &= \frac{\partial T}{\partial r} \\ \frac{\partial T}{\partial \Psi} &= \frac{\partial T}{\partial v_x}v_y - \frac{\partial T}{\partial v_y}v_x \end{aligned} \tag{2.3}$$

Deriving a set of Lagrangean equations for the body-fixed frame velocities yields

$$\begin{aligned} \frac{d}{dt}\frac{\partial T}{\partial v_x} - r\frac{\partial T}{\partial v_y} &= Q_{v_x} \\ \frac{d}{dt}\frac{\partial T}{\partial v_y} + r\frac{\partial T}{\partial v_x} &= Q_{v_y} \\ \frac{d}{dt}\frac{\partial T}{\partial r} - v_y\frac{\partial T}{\partial v_x} + v_x\frac{\partial T}{\partial v_y} &= Q_r \\ \frac{d}{dt}\frac{\partial T}{\partial \dot{\varphi}} - \frac{\partial T}{\partial \varphi} + \frac{\partial U}{\partial \varphi} &= Q_\varphi \\ \frac{d}{dt}\frac{\partial T}{\partial \dot{\theta}} - \frac{\partial T}{\partial \theta} + \frac{\partial U}{\partial \theta} &= Q_\theta \end{aligned} \tag{2.4}$$

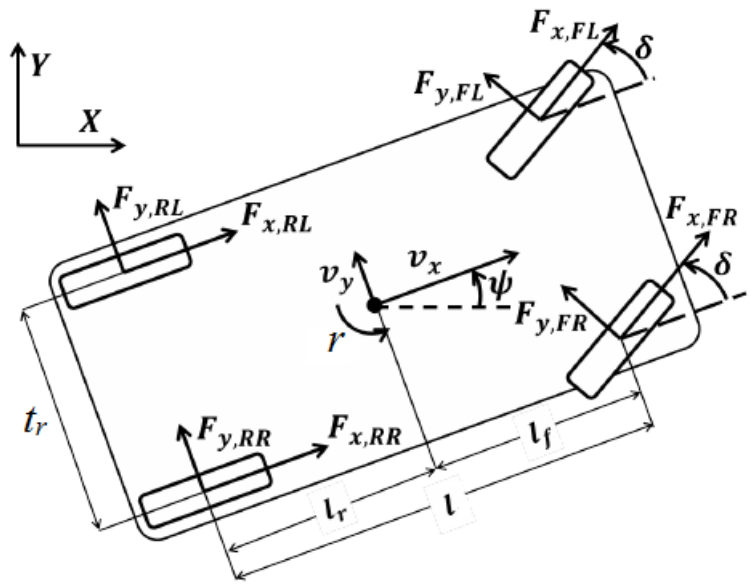

Figure 2.2: Vehicle plane motion

Furthermore, the forces acting on the vehicle can be written as follows.

$$\begin{aligned} Q_{v_x} &= \Sigma F_x = F_{x_1}\cos\delta - F_{y_1}\sin\delta + F_{x_2} \\ Q_{v_y} &= \Sigma F_y = F_{x_1}\sin\delta + F_{y_1}\cos\delta + F_{y_2} \\ Q_r &= \Sigma M_z = l_f F_{x_1}\sin\delta + l_f F_{y_1}\cos\delta + M_{z_1} - l_r F_{y_2} + M_{z_2} \\ Q_\varphi &= -(C_{\varphi_1} + C_{\varphi_2})\dot{\varphi} \\ Q_\theta &= -C_\theta\dot{\theta} \end{aligned} \tag{2.5}$$

where C_{φ_1} and C_{φ_2} are equivalent damping coefficients of the front and rear axle, respectively. Also C_θ represents the equivalent damping coefficient of vehicle pitch motion. Since the terms regarding the presence of inclination angle are small they have been considered to be zero. The equations are linearised in the assumed small roll angle φ and pitch angle θ.

$$\cos\theta \approx 1,\ \sin\theta \approx \theta \tag{2.6}$$

$$\cos\varphi \approx 1,\ \sin\varphi \approx \varphi \tag{2.7}$$

Hence, the kinetic energy T and potential energy U can be written as

$$\begin{aligned} T = {} & \frac{1}{2}m\left((v_x + h'\varphi r + h''\dot{\theta})^2 + (v_y - h'\dot{\varphi} + h''\theta r)^2\right) + \frac{1}{2}I_{xx}\dot{\varphi}^2 + \frac{1}{2}I_{yy}(\varphi r)^2 + \frac{1}{2}I_{yy}\dot{\theta}^2 + \ldots \\ & \frac{1}{2}I_{xx}(r\theta)^2 + \frac{1}{2}I_{zz}r^2 - \frac{1}{2}I_{zz}(\varphi^2 r^2 + r^2\theta^2) \end{aligned} \tag{2.8}$$

$$U = \frac{1}{2}(K_{\varphi_1} + K_{\varphi_2})\varphi^2 - \frac{1}{2}mgh'\varphi^2 + \frac{1}{2}K_\theta\theta^2 - \frac{1}{2}mgh'\theta^2 \tag{2.9}$$

where K_{φ_1} and K_{φ_2} are considered to be the front and rear axle roll stiffness, respectively. To simulate the pitch motion, K_θ is used as pitch stiffness. After eliminating the negligible terms,

Table 2.1: Vehicle states

State	Symbol
Longitudinal velocity	v_x
Lateral velocity	v_y
Yaw rate	r
Roll rate	$\dot{\varphi}$
Roll angle	φ
Pitch rate	$\dot{\theta}$
Pitch angle	θ

the final equations of motion can be established.

$$
\begin{aligned}
&m(\dot{v_x} - rv_y + h'\varphi\dot{r} + 2h'\dot{\varphi}r + h''\ddot{\theta} - h''\theta r^2) = Q_{v_x}\\
&m(\dot{v_y} + rv_x - h'\ddot{\varphi} + h'r^2\varphi + 2h''\dot{\theta}r + h''\theta\dot{r}) = Q_{v_y}\\
&I_{zz}\dot{r} + mh'(\dot{v_x} - rv_y)\varphi + mh''(\dot{v_y} + rv_x)\theta = Q_r\\
&(I_{xx} + mh'^2)\ddot{\varphi} - mh'(\dot{v_y} + rv_x) - (mh'^2 + I_{yy} - I_{zz})r^2\varphi - mh'h''(\theta\dot{r} + 2\dot{\theta}r) + (K_{\varphi_1} + K_{\varphi_2} - mgh')\varphi = Q_\varphi\\
&(I_{yy} + mh''^2)\ddot{\theta} + mh''(\dot{v_x} - v_y r) - (mh''^2 + I_{xx} - I_{zz})r^2\theta + mh'h''(\dot{r}\varphi + 2r\dot{\varphi}) + (K_\theta - mgh'')\theta = Q_\theta
\end{aligned}
\tag{2.10}
$$

Solving these equations will give the states of the vehicle. Table 2.1 shows the parameters of the vehicle states with their descriptions

2.2 Longitudinal model

Although there is a 5-DOF vehicle model developed, but in order to implement a model into a longitudinal controller which will be added to the vehicle by the company, a simplified model of the vehicle is sufficient due to necessity of real-time implementation. In the first part the longitudinal model is explained which is followed by the identification of the unknown model parameters.

2.2.1 Modeling

The longitudinal dynamics of the vehicle on a flat road are given by

$$\dot{v_x} = \frac{1}{m}\Big(\frac{T_e.i_F.i_G}{r_w} - \frac{1}{2}\bar{\rho}C_dA_fv_x^2 - F_{rol}\Big) + v_y r \tag{2.11}$$

where v_x and v_y are longitudinal velocity (m/s) and lateral velocity (m/s), respectively. m is the vehicle mass (kg) and T_e is the engine torque (N.m). Wheel radius (m) is shown as r_w and $\bar{\rho}$ shows air density (kg/m^3).C$_d$ is the symbol for drag coefficient and A_f presents the frontal area (m^2).F$_{rol}$ is the rolling friction force (N) and r is yaw rate (rad/s). i_F and i_G are final drive ratio and gear ratio, respectively.
Eliminating the rolling friction force because of its small value at high vehicle velocities, the model can be simplified to consist the force coming from the engine torque and the air drag force.

$$\dot{v_x} = \frac{1}{m}\Big(\frac{T_e.i_F.i_G}{r_w} - \frac{1}{2}\bar{\rho}C_dA_fv_x^2\Big) \tag{2.12}$$

Having a certain velocity profile, this model is capable of finding the required engine torque. In other words, the model can be used to determine the input torque depending on the reference longitudinal velocity. More information about the implementation of this model for longitudinal velocity control can be found in Section 4.2.

2.2.2 Identification

The parameters for the simplified longitudinal model are shown in Table 2.2.

Table 2.2: Longitudinal model parameters

Longitudinal model parameters		
Parameter	Resource	Value
Vehicle mass (m)	Datasheet	3468 kg
Wheel radius (r_w)	195/75R16C tire	0.35 m
Drag coefficient (C_d)	Forums and websites	0.34 $-$ 0.36
Frontal area (A_f)	0.84*width*height [3]	4.5034 m^2

Using the parameter values, the model can be used to control the input torque depending on the reference longitudinal velocity.

2.3 Handling model

In this study, single track model, also known as bicycle model, is used to obtain the tire parameters as shown in Figure 2.3. The reason is that with the available data from the sensors, it is only possible to obtain the cornering stiffness for the front and rear axle (and not for each wheel separately). The equations of motion for this model are as follows

$$m(\dot{v_y} + v_x r) = F_{y_f} + F_{y_r} \tag{2.13}$$

$$I_{zz}\dot{r} = l_f F_{y_f} - l_r F_{y_r} \tag{2.14}$$

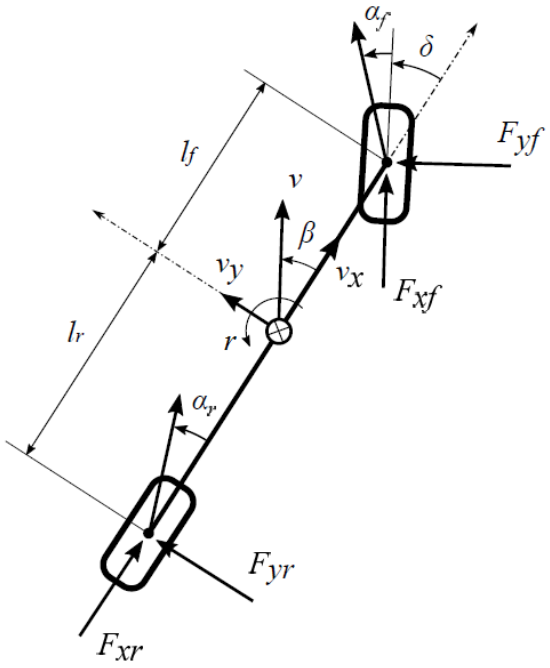

Figure 2.3: Bicycle model

where F_{y_f} and F_{y_r} are the lateral force acting on the front and rear (lumped) wheels, respectively.

2.4 Rotational model

In order to estimate the roll and pitch parameters of a vehicle, linear second order model (spring-damper-mass system) is used for the estimation [9].

2.4.1 Roll model

Although the suspension travel has some effects on measuring the roll stiffness and damping, but it is shown that a linear second order model for roll motions gives very close results to measurements obtained by real tests [8].

$$I_{xx}.\ddot{\varphi} + C_{\varphi}.\dot{\varphi} + K_{\varphi}.\varphi = m.a_y.\delta_h + m.g.\delta_h.\varphi \tag{2.15}$$

where δ_h is the distance between roll center and center of mass.

2.4.2 Pitch model

The same concept used for roll model can be applied to the pitch model. A linear second order model is used for pitch parameter estimation.

$$I_{yy}.\ddot{\theta} + C_{\theta}.\dot{\theta} + K_{\theta}.\theta = m.a_x.\delta_{h'} + m.g.\delta_{h'}.\theta \tag{2.16}$$

in which $\delta_{h'}$ is the distance between pitch center and center of mass.

2.5 Wheel dynamics

Wheel angular velocity can be obtained by writing the moments applied on the wheel. Braking torque, drive torque (torque applied to the wheels by the engine) and the moment acting on the contact patch are the three moments that are considered for this study as shown in Figure 2.4 and can be expressed as follows [2]

$$I_w\dot{\omega} = T_w - M_b - F_{x,rr}r_w \tag{2.17}$$

where $F_{x,rr}$ is the force due to rolling resistance. Hence, by doing an integration in the model, the wheel angular velocity is calculated.

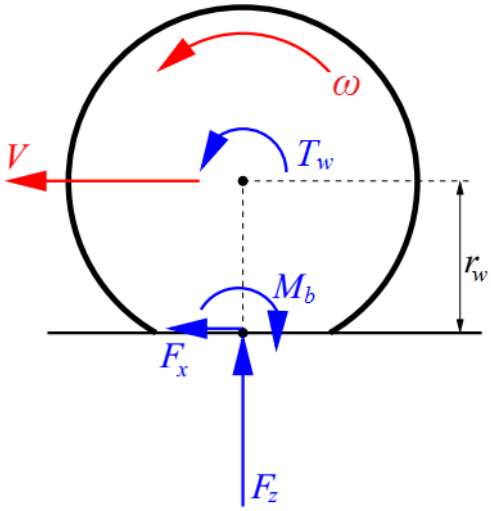

Figure 2.4: Wheel dynamics [2]

2.6 Slip calculation

Longitudinal and lateral Slip relations are shown in Equation 2.18 and 2.19, respectively [2].

$$\kappa = -\frac{V_x - \omega r_w}{V_x} \tag{2.18}$$

$$\alpha = \arctan(\frac{V_{sy}}{V_x}) \tag{2.19}$$

In which V_x and V_{sy} are longitudinal and lateral velocity of each wheel in wheel-mounted coordinate axes.

2.7 Tire model

There are many tyre models than can be implemented in a vehicle model. However, depending on the desired accuracy and computational time, as well as data availability, the choice can be made. In this study, two different tyre models have been considered because of their ability to model the non-linear tire regime and also the simplicity of their parameters: Dugoff tire model and Pacejka tire model (Magic Formula).

2.7.1 Dugoff tire model

It is shown that Dugoff tire model provides a reasonable trade off between accuracy for fitting the model and computational load with respect to other tire models [4].
The tire forces are given by

$$F_x = C_\sigma \frac{\sigma_x}{1+\sigma_x} f(\lambda) \tag{2.20}$$

$$F_y = C_\alpha \frac{\tan(\alpha)}{1+\sigma_x} f(\lambda) \tag{2.21}$$

where λ is calculated as

$$\lambda = \frac{\mu F_z (1+\sigma_x)}{2\left((C_\sigma \sigma_x)^2 + (C_\sigma \tan(\alpha))^2\right)^{0.5}} \tag{2.22}$$

and

$$f(\lambda) = 1 \text{ if } \lambda < 1 \tag{2.23}$$
$$f(\lambda) = (2 - \lambda)\lambda \text{ if } \lambda \geq 1 \tag{2.24}$$

Also depending on braking or accelerating, the theoretical longitudinal tire slip can be calculated as follows

$$\begin{cases} \sigma_x = \dfrac{V_x - r_w\omega}{V_x} \text{ if braking} \\ \sigma_x = \dfrac{r_w\omega - V_x}{r_w\omega} \text{ if accelerating} \end{cases} \tag{2.25}$$

2.7.2 Pacejka tire model (Magic Formula)

Tires are the most difficult component of a vehicle to model. However, their modeling plays a key role in the whole vehicle model. The magic tire formula proposed by Pacejka is probably the most popular tire model for vehicle simulations. Figure 2.5 shows an overview of the model inputs and outputs [2]. In this study, one of the most simple form of magic formula employing 14 parameters is used [4]. However, due to lack of some measurement tools and to simplify the calculations, the camber angle effect and aligning moment are neglected. It should be mentioned that assumed model to use magic formula is the bicycle model as shown in Figure 2.3.

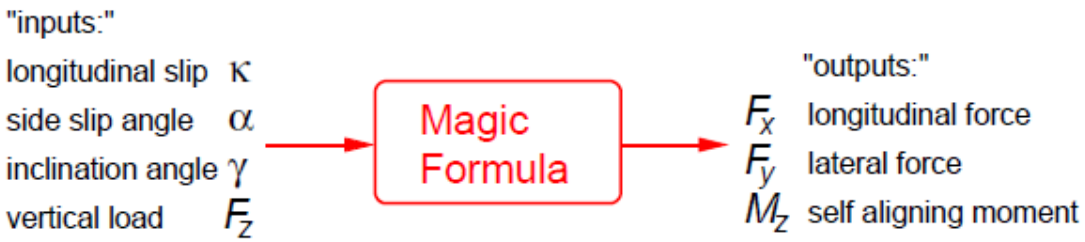

Figure 2.5: Magic formula functional overview

$$F_x = (F_z D_x) \sin\Big(C_x \arctan\big(B_x(1 - E_x)\kappa + \arctan(B_x\kappa)\big)\Big) \tag{2.26}$$
$$F_y = (F_z D_y) \sin\Big(C_y \arctan\big(B_y(1 - E_y)\alpha + \arctan(B_y\alpha)\big)\Big) \tag{2.27}$$

where F_z is obtained for each axle using the bicycle model.

$$F_{z_f} = mg\frac{l_r}{l_r + l_f} - a_x m h_{CG} \tag{2.28}$$
$$F_{z_r} = mg\frac{l_f}{l_r + l_f} + a_x m h_{CG} \tag{2.29}$$

Using a small angle approximation, the front and rear side slip angles are given by:

$$\alpha_f = \frac{v_y + l_f\dot{\phi}}{v_x} - \delta \tag{2.30}$$
$$\alpha_r = \frac{v_y - l_r\dot{\phi}}{v_x} \tag{2.31}$$

Chapter 3

Parameters and computational methods

In order to adapt the model with other simulation software such as preScan, it is required that the model be created in MATLAB/Simulink software. Overview of the Simulink model can be seen in Figure 3.1. It is worth noting that either the Dugoff tire model or Pacejka tire model can be used in the Simulink model. In this study, however, the Dugoff tire model has been chosen to be implemented because of lack of measurements to identify the Pacejka tire model parameters.

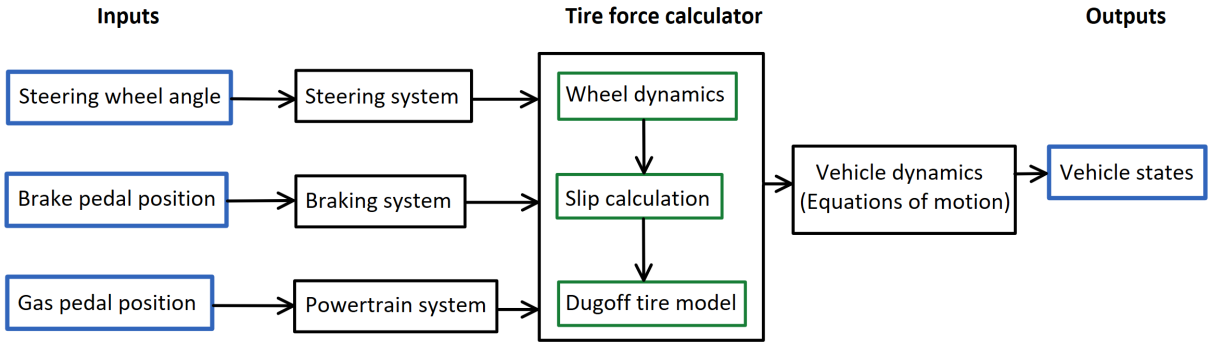

Figure 3.1: Overview of the Simulink model

Table 3 shows the inputs, constants and outputs of the system.

Table 3.1: System inputs, outputs and constant parameters

Simulink model		
Inputs	Constants	Outputs
Steering angle (δ)	Wheelbase (L)	Longitudinal velocity (v_x)
Wheel torque (T_w)	Mass (m)	Lateral velocity (v_y)
Brake Torque (M_b)	Moment of Inertia (I_{xx}, I_{yy}, I_{zz})	Yaw rate (r)
	CG location (l_f, h_{CG})	Side slip angle (β)
	Track width (t_f, t_r)	Roll angle (φ)
	Roll center height (h')	Pitch angle (θ)
	Pitch center height (h'')	Long. acceleration (a_x)
	Roll stiffness (K_{φ_1}, K_{φ_2})	Lat. acceleration (a_y)
	Pitch stiffness (K_θ)	Longitudinal slip (κ)
	Roll damping (C_{φ_1}, C_{φ_2})	Lateral slip (α)
	Pitch damping (C_θ)	Vehicle velocity (V)
	Tyre radius (r_w)	Tyre forces (F_x, F_y, F_z)
	Wheel moment of inertia (I_w)	

The Simulink model is mostly based on the first chapter of Prof. Pacejka's book [10] and the overall model structure was provided by Dr. Besselink during his course on Vehicle Dynamics at Eindhoven Unversity of Technology (2015) [2].

3.1 Parameters estimation

Some constant parameters for the Mercedes Benz Sprinter can be obtained from the datasheet provided by the manufacturer or some rule of thumbs. The remaining parameters need to be identified by experiments in the next chapter.

Table 3.2 shows the estimated parameters together with their source. There are explanations in the following subsections in order to clarify the rule of thumbs and approximations for some of the parameters.

Table 3.2: Parameters estimation overview

Parameters estimation overview		
Parameter	Source	Value
Vehicle mass (m)	Datasheet	3468 kg
Wheelbase (L)	Datasheet	4.325 m
Track width (t_f, t_r)	Datasheet	1.708 m
Rear roll center height (h_2')	Rule of thumb	0.46 m
Pitch center height (h'')	Rule of thumb	0.40 m
Moment of inertia (I_{xx}, I_{yy}, I_{zz})	Approximation formula	$1858, 11933, 11933 kg.m^2$
Wheel radius (r_w)	Datasheet	0.35 m
Wheel moment of inertia (I_w)	Approximation formula	$m_w\, r_w^2$
Final drive ratio (i_F)	Datasheet	0.53
Gear ratio (1-6) (i_G)	Datasheet	$4.38, 2.86, 1.92, 1.37, 1, 0.82$

3.1.1 Rear roll center and pitch center height

For the rear axle, it is mentioned that connecting the two points that the leaf spring is joint to the body and intersecting it with the vertical line that goes through the wheel center can determine the rear roll center height. Experiments have confirmed the validation of this method to obtain roll center height for leaf spring suspensions [7].

For the studied vehicle, the rear roll center height is measured approximately.

$$h_2' = 0.46 \text{ m} \tag{3.1}$$

Unfortunately, for pitch center, there is no specific procedure to obtain the pitch center height. Hence, based on some database for different vehicles, this value is estimated. However, it may be tuned after the experiments.

$$h'' = 0 \text{ m} \tag{3.2}$$

3.1.2 Moment of inertia approximation

Since the measurement setup for finding moment of inertia is expensive and it is not possible to achieve enough excitations with the bus in order to identify the moment of inertia, approximated values are used for moment of inertia. In [6], there are two rules of thumb mentioned in order to achieve each moment of inertia. Although the inputs are in US units, the conversion ratio is provided in order to obtain equivalent SI values.

$$1\ ft.lb.sec^2 = 1.35582\ kg.m^2 \tag{3.3}$$

First method - Considering shape and mass distribution: Since the test vehicle in this project can be categorized as light trucks, the following estimations are provided regarding to that

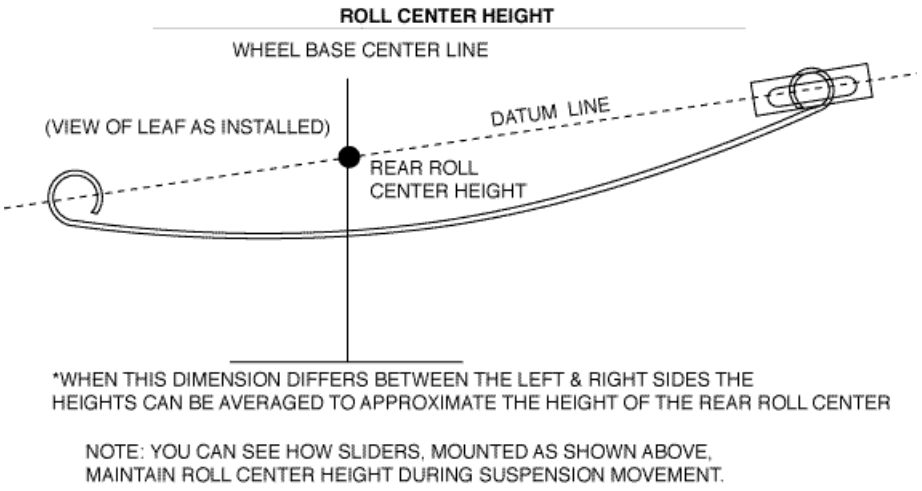

Figure 3.2: Leaf spring roll center height [1]

category. However, due to the great diversity of such vehicles (pickup, van, multi-purpose vehicle), these estimation may not be accurate.

$$I_{zz} = I_{yy} = m.l_f.l_r \quad \text{in US units} \tag{3.4}$$

$$I_{xx} = 0.67m.\frac{t_f + t_r}{8}.H_r \quad \text{in US units} \tag{3.5}$$

In which m is the vehicle mass and H_r is the roof height.

Second method - Weight only: Second method provides a more general approximation for a light-truck vehicle. The mentioned reference computed regression correlation coefficient of 0.70 to 0.73 which shows this estimation is not accurate due to the scattered data.

$$I_{zz} = 1.03\,W - 1343.0 \quad \text{in US units} \tag{3.6}$$

$$I_{yy} = 1.12\,W - 1657.0 \quad \text{in US units} \tag{3.7}$$

$$I_{xx} = 0.22\,W - 235.0 \quad \text{in US units} \tag{3.8}$$

In which W is the vehicle weight.
Using the second is useful when the vehicle is in the category of light trucks (e.g. Ford F150). The results obtained from this method were not intuitive. The numbers were close to pick-ups but intuitively, they have to be higher due to larger inertia of minibus. Hence, the first method results is used in this study in order to achieve an approximation for the moment of inertia.

Results: Table 3.3 shows the result for the moment of inertia.

Table 3.3: Moment of Inertia approximation using the mentioned methods

First method	
Moment of Inertia	$kg.m^2$
I_{xx}	1858
I_{yy}	11933
I_{zz}	11933
Second method	
I_{xx}	1444
I_{yy}	6891
I_{zz}	6518

Chapter 4

Experiments

4.1 Introduction

In order to obtain the remaining unknown vehicle parameters, it is necessary to estimate the constant values using experimental setup and field tests.

4.1.1 Test vehicle

The internship assignment was to model and identify the test vehicle. The vehicle was a 2014 Mercedes Benz Sprinter 513 CDi (Figure 4.1) which belonged to VDL Bus and Coach Belgie and its driving has to be automated. Very few parameters of the vehicle where directly available from the provider datasheet and hence, some test had to be performed to identify non-available parameters using the available equipment that is mentioned in the next subsection. Moreover, due to some limitations such as setup availability, cost issues and time limitation, some tests were not feasible to run.

4.1.2 Equipment

There were several devices available at the company to use for the designed tests and obtaining the model parameters. Those that are used for this study have been briefly explained.

Inertial Navigation and Global Positioning based systems

The INS device provides a tactical grade accuracy on vehicle states (velocities, accelerations, rotations, etc.) in a compact package. It included an IMU and an on-board enhanced EKF. The available model had two GPS antenna receivers to achieve the best accuracy by integrating data from GPS, Odometer, etc.

Drive by wire

Drive by wire, Steer-by-wire, or x-by-wire technology in the automotive industry is the use of electrical or electro-mechanical systems for performing vehicle functions traditionally achieved by mechanical linkages. However, the usage of such system in this study is to have rather accurate inputs for the gas pedal/brake pedal position and also the steering wheel. Hence, by electronically inserting the equivalent values, the system actuates the gas pedal, brake pedal and steering wheel.

Non-contact optical sensors

The 2-axis sensors are designed for direct, slip-free measurement of longitudinal and transverse vehicle dynamics. Longitudinal and lateral velocities can be obtained by this sensor which can also be used to calculate the side slip angle.

Figure 4.1: Mercedes Benz Sprinter at Flanders Make

4.2 Identification experiments

Table 4.1 shows the parameters that need to be found experimentally with their related experiments. Following sections will describe the experiments in detail.

Table 4.1: Identification experiments

Parameter Identification by Experiments	
CG distance (l_f)	Weight the vehicle on each axle
CG height (h_{CG})	Weight the vehicle with lifted front
Torque to Gas pedal position conversion (T_e)	Dyno test (or straight driving)
Roll center height (h')	2 post hoist and front suspension travel
Roll stiffness (K_{φ_1}, K_{φ_1}) Roll damping (C_{φ_1}, C_{φ_1})	Constant radius test (or step steering test)
Pitch stiffness (K_θ) Pitch damping (C_θ)	Emergency braking test (no steering)

4.2.1 Torque to gas pedal position conversion

In longitudinal control, there has to be a conversion from wheel torque to gas pedal position in order to being able to insert the user-input (drive by wire system here) into the system. The obtained look up table will be the connection between the controller and the drive by wire system which controls the gas pedal. (Figure 4.2)

The most accurate result can be obtained by performing the dyno test and using the acquired result. However, due to the limited internship time interval, this was not feasible at the time. Hence another test was designed and implemented.

Usage of the parameter:

- Finding the equivalent gas pedal position for longitudinal controller
- Conversion from Gas pedal position to wheel torque in Simulink model

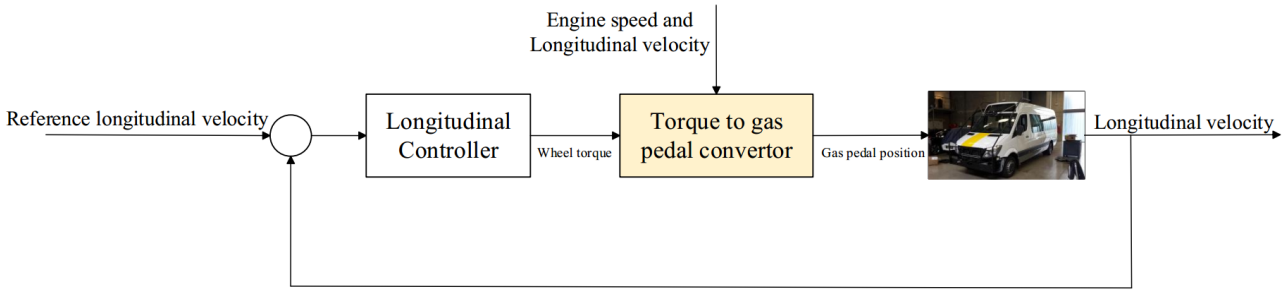

Figure 4.2: Longitunial control overview

Required setup:

- IMU+GPS (INS) (for longitudinal acceleration)
- Optical sensor (for longitudinal velocity)
- Drive by wire (for gas pedal position and engine speed)

Theory: As explained in Section 2.2.1, the *engine torque* can be calculated using the *acceleration*, *velocity* and *gear ratio*. To obtain the torque-speed characteristics of the engine, it is necessary to make a look up table containing the *engine torque*, *engine speed* and *gas pedal position*. Hence, knowing the *required torque* and current *engine speed*, the related *gas pedal position* will be acquired. Figure A.5 shows this look-up-table. Moreover, there should be a mechanism to detect the current gear in order to being able to insert the correct gear ratio. In fact, the current gear is obtained by dividing RPM (engine speed) by vehicle velocity data and compare it with the gear ratios (multiplied by the final drive ratio).

$$T_w = m.a_x \tag{4.1}$$
$$T_w = T_e.i_G.i_F - T_{\text{friction}} - T_{\text{air drag}} \tag{4.2}$$

It should be mentioned that other torque losses for example torque due to the center of gravity changing and transmission losses are neglected.

Friction torque is mostly due to the rolling resistance which is dominant in low speeds. *Rolling resistance force* is because of the fact that as the tires rotate, the normal force distribution on the tires moves a bit forward on the contact patch and hence opposes the rotating direction. This resistance force is assumed to have a linear relation with the normal force. The following equation shows their relation [11].

$$F_R = f_R.F_z \tag{4.3}$$
$$T_{friction} \approx F_R.r_w \tag{4.4}$$

In which f_R is the rolling resistance coefficient.

Result: Using the relations above and measuring the engine speed and gas pedal position real-time data, it now becomes possible to use the look-up-table and find the required gas pedal position in order to reach a certain acceleration (or wheel torque). Figure A.5 shows the final result.

4.2.2 Brake torque to brake pedal position conversion (braking system look-up table)

Although the vehicle brake dynamics can be heavily dependent on the environment situation e.g. road surface friction and brake fluid temperature, a look up table consisting of the brake pedal position (drive-by-wire system input) and vehicle longitudinal acceleration can be made in order to have approximated results that can be implemented in the longitudinal controller.

Usage of the parameter:

- Finding the required brake pedal position for longitudinal controller
- Conversion from brake pedal position to wheel torque in Simulink model

Required setup:

- IMU+GPS (INS) (for **longitudinal acceleration**)
- Drive by wire (for **brake pedal position**)

Test Procedure: The results obtained from the Kristal Park test for longitudinal controller can also be used here. A 1-D look up table from brake pedal position (drive by wire system input) to (negative) wheel torque can be made and implemented on the longitudinal controller in parallel to the engine look up table.

4.2.3 Calculating the center of gravity location

Usage of the parameter:

- In many model formulas such as in equation of motion, roll and pitch simulation, etc.

Required setup:

- Independent scales
- 2 post hoist

Theory: In this section, the procedure for calculating the location of center of gravity is explained. A static test needed to obtain normal forces at each wheel. However, it is assumed that The vehicle is symmetric about a longitudinal plane of symmetry. Vehicle is weighted on a scale in two different positions shown in Figure 4.3 and Figure 4.4.

Before the measurement was taken, the tires were inflated to maximum pressure and the vehicle suspension at the front and rear axle was locked (or shock absorbers was replaced by solid links) to prevent errors due to suspension travel. The axle loads Wf_1 and Wr_1 are weighted when the vehicle is on a flat (horizontal) surface. Similarly, Wf_2 and Wr_2 are measured when one axle is raised by amount of "a". It is recommended that $a = 500mm$ for this vehicle [13].
Since the vehicle is in static position, the summation of all moments about a point must be zero. Therefore, the center of gravity distance from rear axle can be calculated as follows

$$xr_1 = \frac{Wf_1.WB_1}{Wf_1 + Wr_1} \tag{4.5}$$

For raised axle test (Figure 4.4), the center of gravity height can be obtained using Equation 4.6.

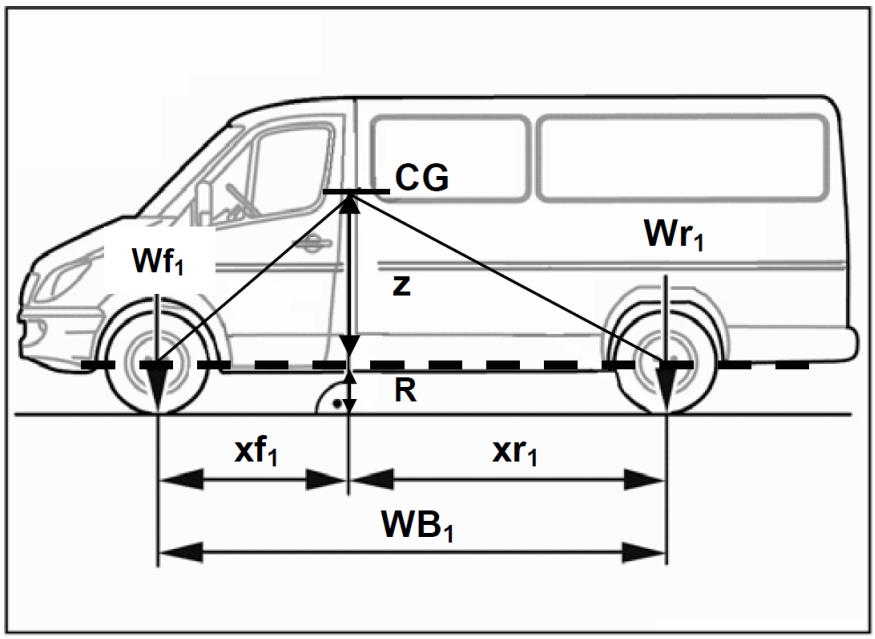

Figure 4.3: Measurement with vehicle level

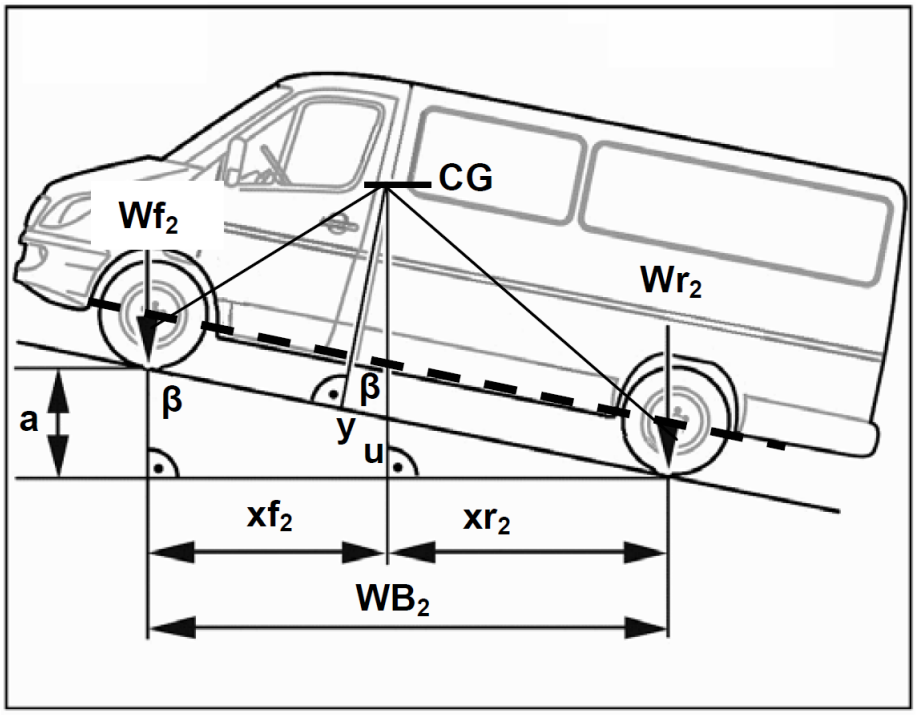

Figure 4.4: Measurement with axle raised

Table 4.2: Center of gravity distance test result

Driver Included				
Wheel position	Left	Right	Total	Distribution
Front	896 kg	879 kg	1775 kg	51.3 %
Rear	878 kg	809 kg	1687 kg	48.7 %
Total			3462 kg	
Without Driver				
Front	859 kg	857 kg	1716 kg	50.7 %
Rear	863 kg	808 kg	1670 kg	49.3 %
Total			3386 kg	

$$h = R + \tan\left(\cos^{-1}\left(\frac{a}{WB_1}\right)\right).\left(\frac{Wf_1.WB_1}{W} - \frac{Wf_2.WB_1}{W}\right) \tag{4.6}$$

In which R is static radius height of front and rear wheels.

Results: The results for level vehicle test with and without driver can be seen in Table 4.2. The test for the lifted vehicle (center of gravity height) was not implemented because the weight scale rental provider did not reply!
Although the vehicle weight on the left and right tires are not exactly the same, the assumption of symmetricity of the vehicle about a longitudinal plane of symmetry is still acceptable.

Using the result, the center of gravity location can be calculated.

$$x_{r_1} = 2192\ mm,\ x_{f_1} = 2133\ mm \text{ with driver and 30\% fuel} \tag{4.7}$$

$$x_{r_1} = 2217\ mm,\ x_{r_1} = 2108\ mm \text{ without driver and 30\% fuel} \tag{4.8}$$

Meaning that driver presence results in 1.17% deviation in CG longitudinal location for the test vehicle.

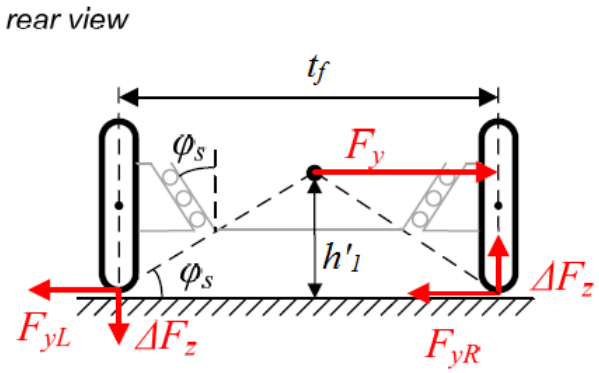

Figure 4.5: Rear view of a single axle considering roll center [2]

4.2.4 Front roll center height approximations

Usage of the parameter:

- Roll motion simulation and load transfer

Required setup:

- 2 post hoist

Theory: In this section, an easy experiment is explained in order to approximate roll center height.
It is shown that there is a relation between support angle φ_s, track width t_f and roll center height h'. (Figure 4.5)

$$\tan(\varphi_s) = \frac{h'}{0.5t_f} \tag{4.9}$$

Since the track width is known, the only parameters that needs to be measured is support angle. To do so, the vehicle body must be lifted in such a way that the body stays level with respect to the ground and the tires still touch the flat. Knowing the amount of lift (displacement in z-direction) and measuring the lateral displacement of tire-road contact (displacement in y-direction), the following equation can be used to obtain the support angle.

$$\tan(\varphi_s) = \frac{\delta_y}{2\delta_z} \tag{4.10}$$

Results: Measuring the track-width for the front tires before and after lifting the minibus is shown in Table 4.3.

Hence, the support angle for front axle can be calculated as follows.

$$\varphi_{s_{front}} = 0.4636 \text{ rad} = 26.57^\circ \tag{4.11}$$
$$\varphi_{s_{rear}} = 0.0555 \text{ rad} = 3.18^\circ \tag{4.12}$$

Using the calculated support angle, front roll center height can be estimated.

$$h'_1 = 0.4276 \text{ m} \tag{4.13}$$

Table 4.3: Roll center test result

Vehicle completely on the ground		
Roll center height	δ_z	δ_{r_t}
Front	0.365 m	1.71 m
Rear	0.365 m	1.75 m
Vehicle lifted		
Front	0.455 m	1.62 m
Rear	0.455 m	1.76 m

For rear roll center height, the approximated height is measured to be 0.46 m above the ground. Which gives an approval that the front roll center height is usually smaller that the rear for a few centimeters.

$$h_2' = 0.46\,\text{m} \tag{4.14}$$

Since it is assumed that rear and front roll center height are equal, the roll center is the average taken by the front and rear center height.

$$h' = 0.44\,\text{m} \tag{4.15}$$

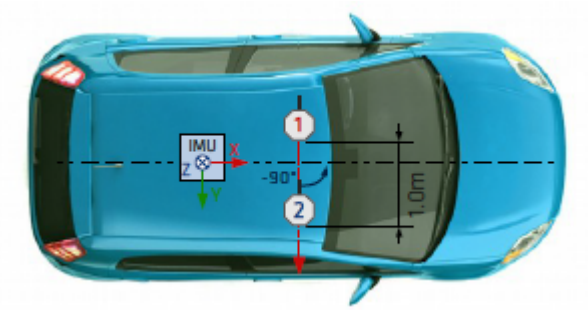

Figure 4.6: Top view of the gps setup for roll parameter estimation

4.2.5 Roll parameter estimation (stiffness and damping)

Usage of the parameter:

- Roll motion simulation and load transfer

Required setup:

- High precision IMU+GPS (roll angle, roll rate, roll acceleration and lateral acceleration)

Thoery: Two antenna GPS setup with INS sensors suggests a distinctive way to estimate roll parameters (roll stiffness and damping) as shown in Figure 4.6. The roll model explained in 2.4.1 is used to estimate the roll parameters.

The roll angle, roll rate and lateral acceleration can be measured using the GPS receiver and INS sensors. However, the roll acceleration can not be measured directly. Hence, numerical differentiation of the roll rate is used to obtain the roll acceleration.
Roll parameters (roll stiffness and damping ratio) can be estimated using a least squares estimator and by exciting the vehicle roll dynamics which can be done by high speed step steering test.

Constant radius test IMU needs to be mounted as close as possible to center of gravity location. GPS antenna positions are shown in the Figure 4.6. Performing a series of constant radius turns at a constant speed, gives (fitted) linear relation between the roll angle and lateral acceleration. The slope of the roll angle vs. lateral acceleration plot is shown in the following equation.

$$\frac{\varphi}{a_y} = \frac{m\delta_h}{K_\varphi - mg\delta_h} \tag{4.16}$$

which can be used to calculate K_φ.
Constant radius test can provide the information for static behaviour of vehicle roll. However, after performing the test, the roll angle did not stay constant during the steady-state part of the maneuver due to malfunctioning of the sensor. Hence, the result of this test has not been used.

Step steering Another method to obtain the roll parameters is to perform a step steering maneuver. This test, however, is practically close to constant radius maneuver. After reaching a certain speed, the test driver excited the roll dynamics of the vehicle by turning the steering wheel by almost 90 degrees.

Implementation Constant radius test maneuver was done at Kristal Park. Unfortunately, the results were not intuitive specially for roll angle due to lack of calibration. Hence, another test at Ford Lommel Proving Ground was done with step steer maneuver. One of the exact test maneuvers is shown in Figure 4.7.

Figure 4.7: Step Steer maneuver implementation at LPG

Results A second order system model for roll motion was created in MATLAB. The parameter estimation toolbox calculates the stiffness and damping of the system based on the lateral acceleration data as input. The (filtered) roll and lateral acceleration data (original) for different speeds and steering input can be seen together with the simulated (fitted) result for roll angle and the average of the all simulations in Figure 4.9 and Figure A.3. Table 4.4 shows the final result for roll parameters. It should be mentioned that due to drift compensation, the roll angle decreased on the turn while the roll acceleration and roll rate stayed almost zero. One probable reason can be that IMU had deducted the drift more than necessary. However, a linear drift compensation has been implemented on the measured data but as shown in Figure 4.8, the roll angle still changes during the steady-state part of the maneuver.

Also, since the suspension model of the vehicle is more complex than a second order system, the results do not perfectly match the expectations. However, the roll angle is obtained by IMU system using the gyro measurements (roll rate). Hence, there can be some errors due to those calculations too. Taking the transient section of the data, the roll parameters can be obtained. (Figure 4.9)

The final estimations which are the average of right and left turn results are as follow:

$$C_\varphi = 2625 \text{ N.s/rad} \tag{4.17}$$

$$K_\varphi = 167375 \text{ N/rad} \tag{4.18}$$

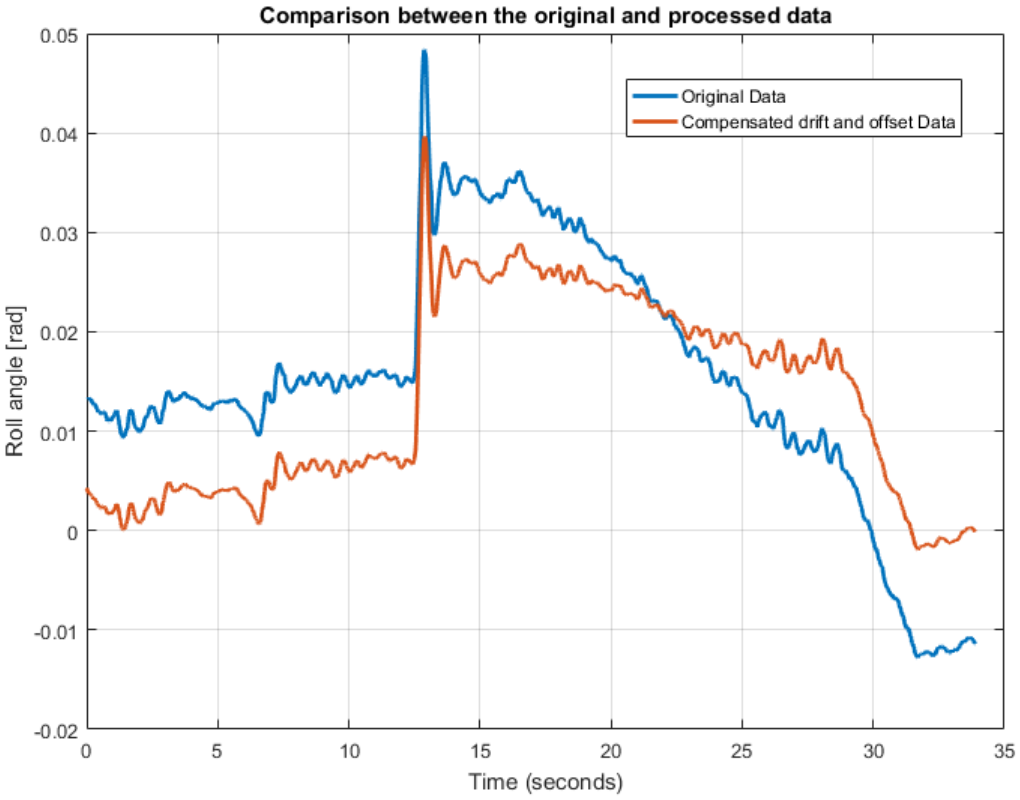

Figure 4.8: Comparison between the raw and processed data for Roll Angle

Table 4.4: Roll parameter test result

Left turn		
Test ID	Roll stiffness (N/rad)	Roll damping (N.s/rad)
Test_0011	169000	2400
Test_0012	167000	2200
Average	168000	2300
Right turn		
Test ID	Roll stiffness (N/rad)	Roll damping (N.s/rad)
Test_0013	166500	3000
Test_0014	167000	2900
Average	166750	2950

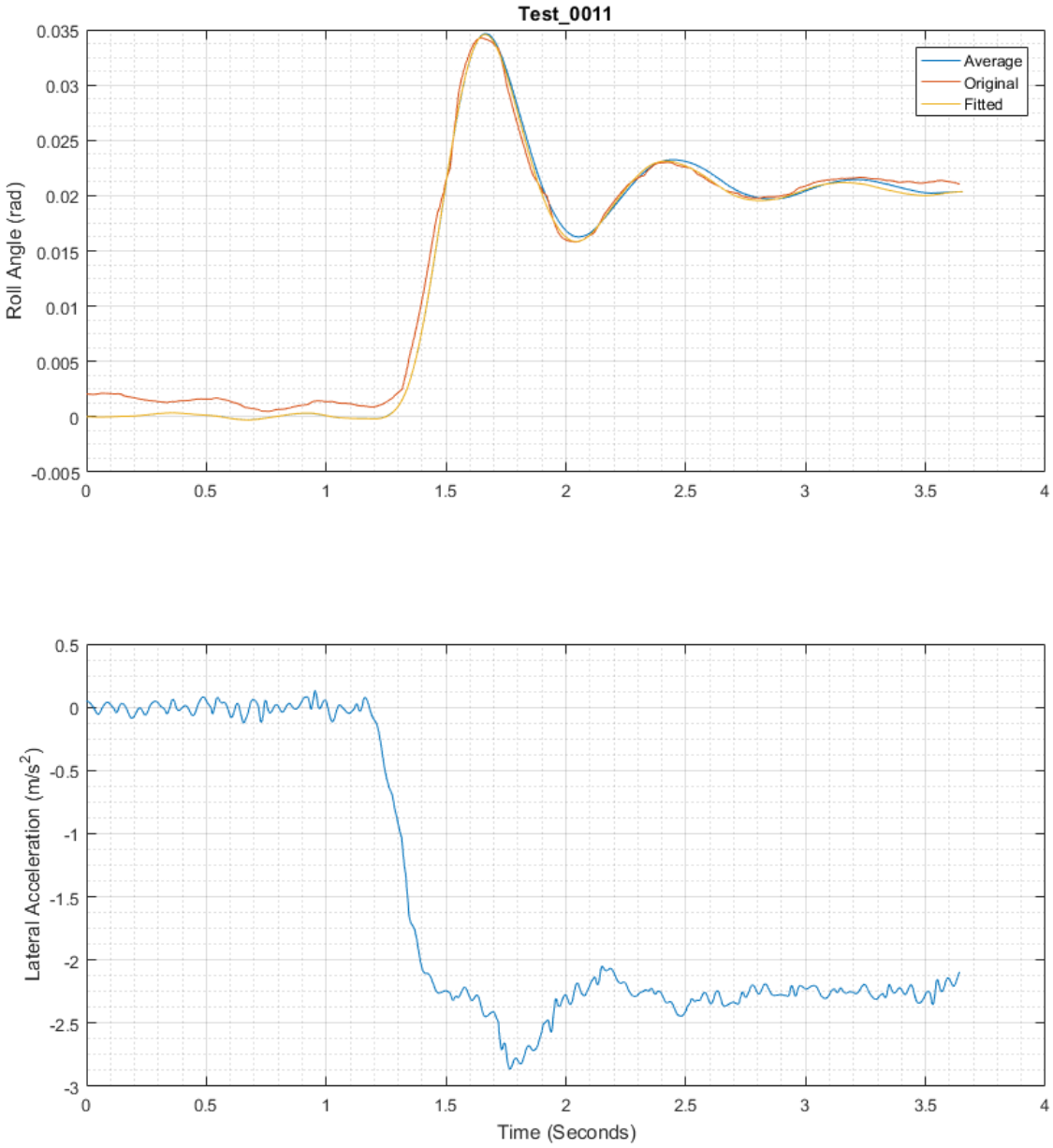

Figure 4.9: Roll parameter estimation result - left turn - low speed and low steering input - Original (filtered) data together with simulated (fitted) data and the average of all the simulations in adapted SAE sign convention system

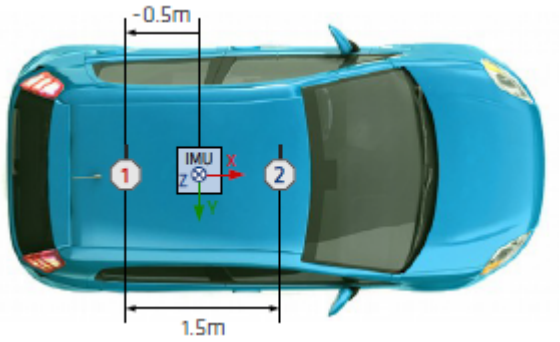

Figure 4.10: Top view of the gps setup for pitch parameter estimation

Table 4.5: Pitch parameter test result

Left turn		
Test ID	Pitch Stiffness (N/rad)	Pitch Damping (N.s/rad)
1	1380000	70000
2	1380000	90000
Average	1380000	80000

4.2.6 Pitch parameter estimation (stiffness and damping)

Usage of the parameter:

- Pitch motion simulation and load transfer

Required setup:

- High cost IMU+GPS (pitch angle, pitch rate, pitch acceleration and longitudinal acceleration)

Thoery: Pitch parameters (pitch stiffness and damping ratio) can be calculated with the same concept as roll parameter estimation. A linear second order system is used as explained in . However, the GPS setup is different in arrangement (Figure 4.10).

The pitch acceleration direct measurement is not possible. In this study, numerical differentiation of the pitch rate presents the roll acceleration. Pitch parameters are approximated using a least squares estimator.

Breaking test (no steering): One way to obtained the pitch parameters is to perform breaking test in which the driver accelerates up to a certain speed in a line and then stops. This maneuver excites pitch dynamics of the vehicle.

Results: After extracting the data from IMU+GPS (SBG systems) and filtering the data using Gaussian filter, the longitudinal acceleration and pitch angle have been considered to obtain the pitch stiffness and damping. Using the System Design Optimization toolbox and estimating the stiffness and damping with Sum Squared Error as the cost function, the results can be acquired. After fine-tuning the parameters for two different tests, the results are given as in Table 4.6. (Figure 6 and 4.11)

$$C_\theta = 80\ kN.s/rad \tag{4.19}$$

$$K_\theta = 138000\ kN/rad \tag{4.20}$$

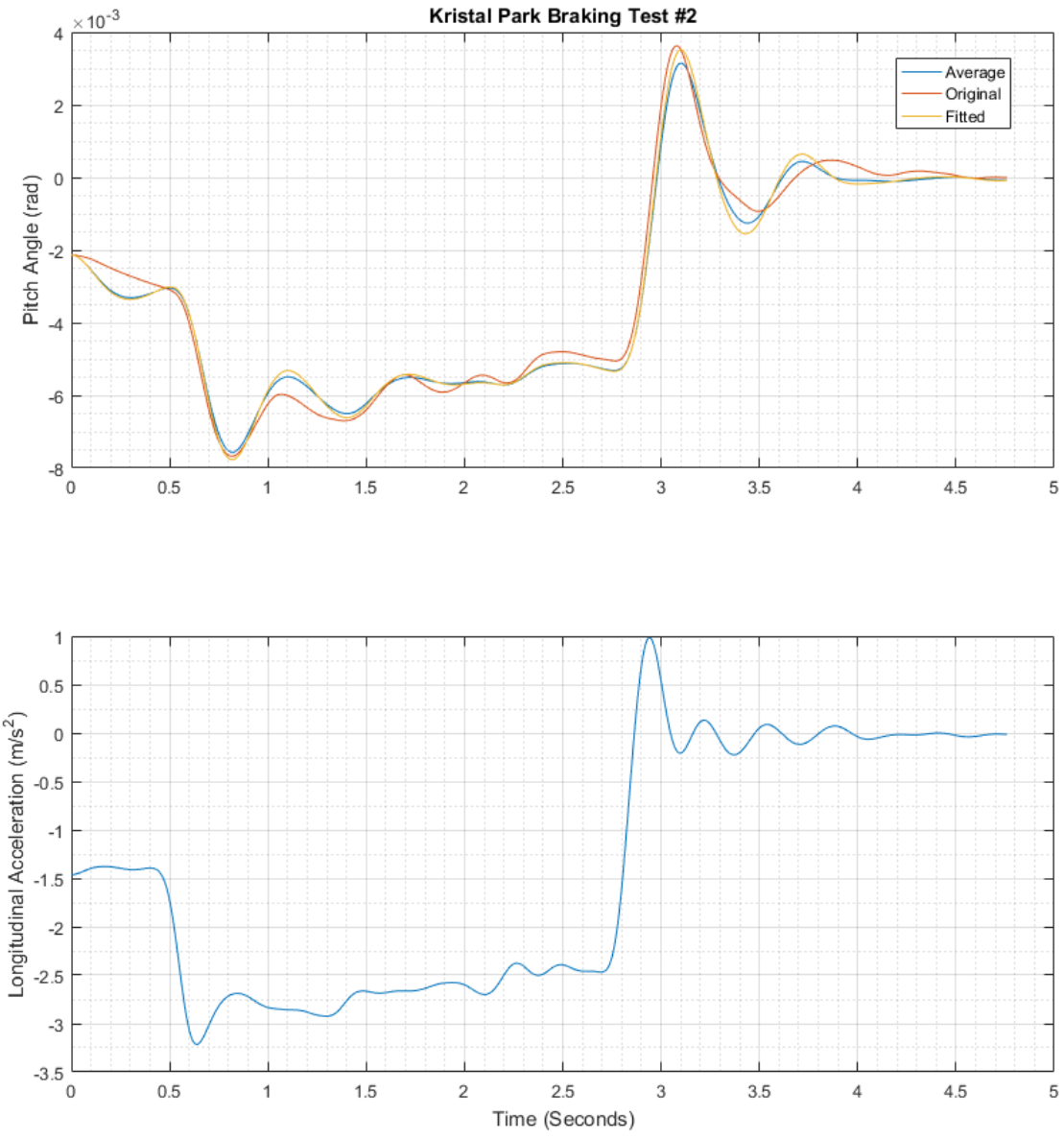

Figure 4.11: Pitch parameter estimation result for MB Sprinter (2) - Original (filtered) measured measured data together with simulated (fitted) data and the average of all the simulations in adapted SAE sign convention system

4.2.7 Dyno test

Usage of the parameter:

- Simulate the longitudinal motion in the complete model
- To calculate the longitudinal slip and obtain the longitudinal tire forces

Required setup:

- Dyno test setup
- Possibility of the gear to be fixed in a certain gear (Tiptronic)
- Cooling fan
- CAN access to engine speed and throttle position

Procedure: The goal of the dyno test in to make a look-up table for throttle position vs engine speed vs engine torque. The table will be used to simulate the tire forces in the complete model.

Prerequisite: One of the inputs of the dyno is the friction coefficient adaption. In order to calculate the engine torque from the wheel torque, the dyno software needs the time intervals of the vehicle naturally slowing down from 100 kph to standstill. This allows the software to adapt the rolling frictions and air drag which exist when the vehicle is on the road. This test was done at Lommel proving ground and the result can be seen in Figure A.7.

Results: Due to limited time of the internship and the malfunctioning of the drive by wire system at the time, this test was not implemented and has been suggested to be done as a future work. The result of this test can be used in the torque to gas pedal conversion (Section 4.2.1) and also in the powertrain system block of the Simulink model.

4.2.8 Tire parameters estimation

Usage of the parameter:

- To obtain the lateral tire forces in the "two track Simulink model"

Required setup:

- Optical sensor to obtain the chassis velocities
- High precision IMU+GPS

Optical sensor needs to be mounted on the front center of the vehicle depending on the space availability.
Same configuration for the high precision IMU+GPS as for the roll parameter experiment.

Ideal theory (future work): The best method to obtain the tire forces is the limit handling test. By doing some maneuvers that take the tire behavior to its "non-linear regime", different tire models can be applied to the obtained experiment data. Magic formula and Dugoff tire model are two of the most famous tire models that is being used in automotive industry.

Limit handling test: Longitudinal acceleration is measured by the high cost IMU+GPS. Hence the normal tire forces can be calculated for the bicycle model. Side slip angles can be approximated using the yaw rate and velocities coming from Correvit S-350 Non-Contact Optical Sensor. Longitudinal slip can be calculated by wheel velocities using the wheel sensors and the wheel velocity approximated using the torque data[1]. All these data points will be fit to the forces obtained by the estimator. However, implementation of this test requires so many safety consideration (e.g. installing safety cages on the vehicle). Hence, it was decided to obtain the tire lateral stiffness within the "linear regime".

Applied theory: If only the linear cornering characteristics of the vehicle are considered, the tire forces can be expressed as follows [2]:

$$F_{y1} = C_1 \alpha_1 \tag{4.21}$$
$$F_{y2} = C_2 \alpha_2 \tag{4.22}$$

In which C_1 and C_2 are the cornering stiffness (N/rad) of the front and rear axle, respectively. Using the single track vehicle track (Bicycle model), the tire lateral forces can be obtained.

$$m a_y = F_{y1} + F_{y2} \tag{4.23}$$
$$I_{zz} \dot{r} = l_f F_{y1} - l_r F_{y2} \tag{4.24}$$

Having the F_{y2}, the lateral cornering stiffness of the rear axle can be obtained using Equation 2.31 and 4.22.
Assuming that the vehicle side slip angle is small, the circle maneuver radius can be obtained using

$$R = \frac{V}{r} \tag{4.25}$$

[1] Longitudinal slip requires Dyno test to be done

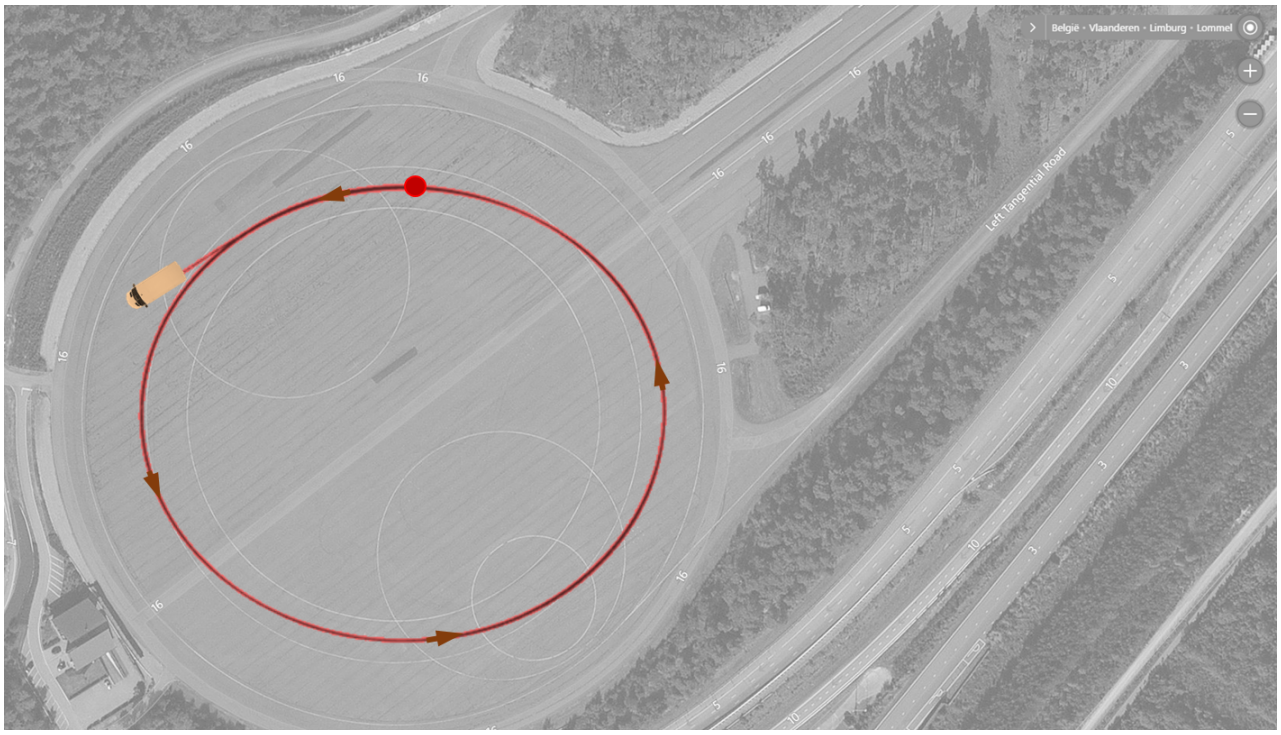

Figure 4.12: Overview of the circle maneuver at LPG (left turn)

where V is the vehicle velocity. Since there was no equipment to directly measure the steering angle position, the required steering angle can be calculated from [2]

$$\delta = \frac{l}{R} - \frac{mV^2}{Rl}(\frac{l_f}{C_2} - \frac{l_r}{C_1}) \tag{4.26}$$

However, C_1 is an unknown on the right side. By using the obtained lateral rear axle force as the update (Equation 4.21), calculation of $C1$ can be put into an iteration.
To extend the model validation, the acquired lateral tire stiffness will be used in Dugoff tire model inside the Simulink model.

Implementation (circle maneuver): To obtain the cornering stiffness of the tires, a constant radius test was implemented at LPG. Since there was no steering angle data collection available at that time, the test driver tried to keep the steady-state cornering situation for as long as possible. The radius was almost 100 meters and velocity was managed to stay at almost 70 kph. (Figure 4.12)

Having the measured lateral acceleration and yaw acceleration, equation 2.13 and 2.14 can be used to obtain the lateral tire forces and the cornering stiffness plots can be achieved. Average of the values in the steady-state interval was taken to be the final values for the mentioned parameters. The obtained values can also be used in Dugoff tire model assuming that Dugoff and linear tire model give almost the same result for linear tire regime. Moreover, Dugoff tire model has the advantage to present the nonlinear regime as well (side slip angle of higher than about 3 degrees).

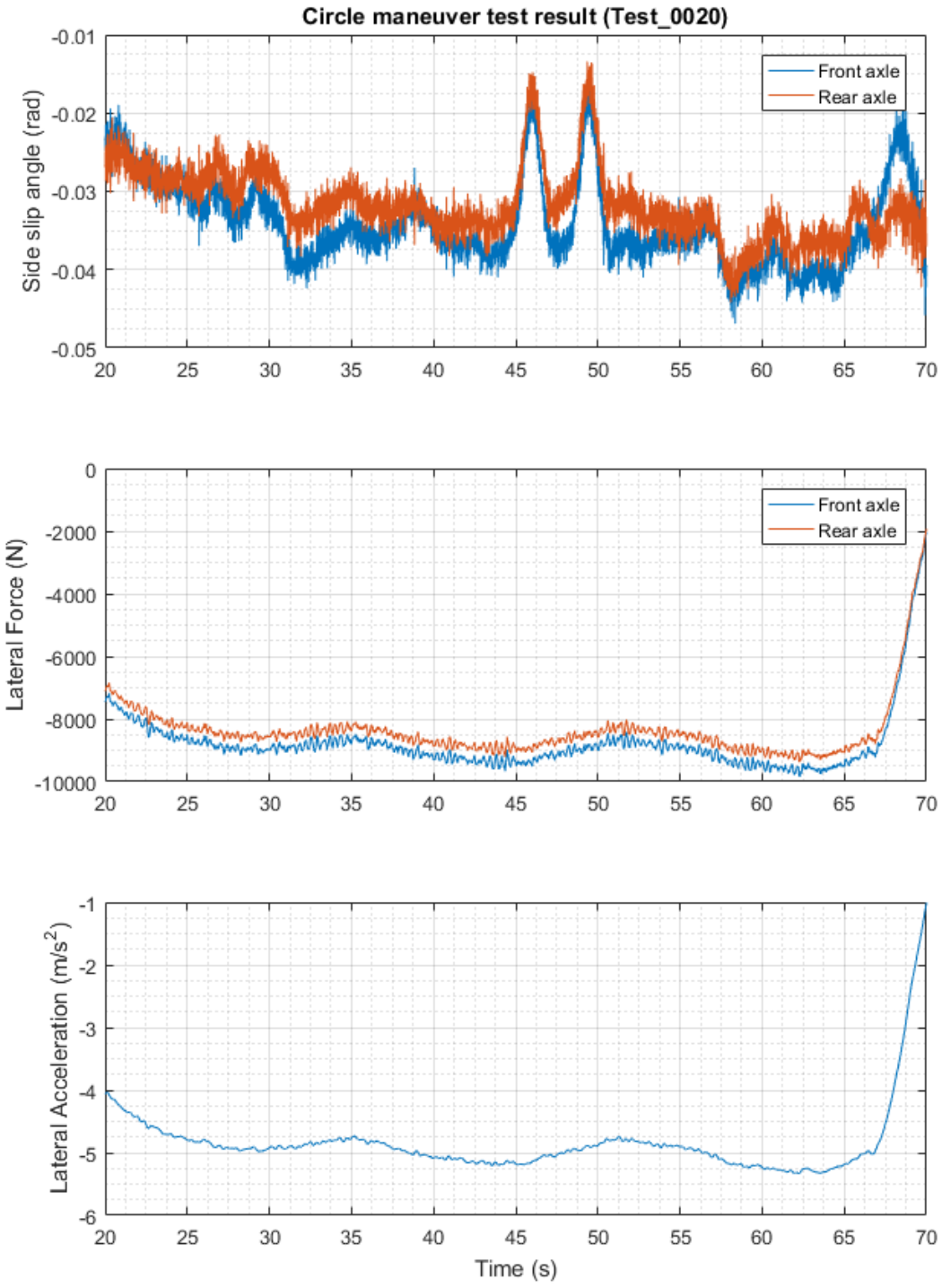

Figure 4.13: Results for circle maneuver test (Test_0020)

Table 4.6: Lateral tire parameter test result

Left turn		
Test ID	C1 (N/rad)	C2 (N/rad)
Test_0019	260000	276000
Test_0020	271000	282000
Average	265500	279000

Chapter 5

Validation

5.1 Validation Experiments

This chapter is dedicated to validate the two track model that has been developed for the urban bus. The identified bus parameters used as constants in the Simulink model. One of the maneuvers that could excite the vehicle dynamics was chosen to be the validation data.(Figure 5.1) Since the sensors used different sign convention than ISO and some components of the Simulink model were in Adapted SAE sign convention system, the final Simulink model is also made in that system and hence, this chapter shows the results using Adapted SAE sign convention.

5.1.1 Step steer maneuver

The step steer maneuver was done at LPG and the sensors measured the states of the vehicle. The vehicle accelerated to a certain speed, after which the test driver abruptly steered and tried to maintained the angle till almost end of the track reached and the vehicle was brought to standstill.

In order to validate the model and compare the results, the model input should be the same as the experiment. Nevertheless, due to lack of accessibility to directly measure the gas and brake pedal as well as the steering angle, those parameters have been simulated in order to match the results as close as possible. The steering wheel rotation, however, estimated using Equation 4.25 and 4.26. In fact, the validation plot regarding the steering angle is actually a comparison between the step input for steering angle and the steering angle obtained from Equation 4.25 and 4.26. Longitudinal velocity plot was chosen to be the measure for gas and brake pedal input. Figure 5.2 to 5.4 show the comparison between the simulation results and raw data from the experiment.

As can be seen, the simulation results are close to what expected. However, there are some mismatch which has to be explained.
As mentioned before, due to lack of gas input measurements, step inputs have created in order to mimic the gas pedal behaviour as close as possible. Although the mismatch can be seen in the longitudinal acceleration graph, but it is believed that even with the non-perfect inputs, the results are comparable to the experiment by an acceptable accuracy. Also, it should be mentioned that around the 35th second, the braking has been simulated by a step input which clearly is not exactly what happened during the experiment. This mismatch has resulted in mismatch of slope for almost all the variables. Moreover, the IMU used to measure the roll and pitch angle did not give intuitive result for those angles because the angles did not stay constant during the steady state part of the maneuver. Firstly, they had too much drift that had to be compensated and secondly, they didn't match with their rate. Hence, roll and pitch rates have been considered.
The author believes that with having accurate inputs (steering angle, gas pedal and brake pedal position), the model is capable of reaching high accurate result specially in linear tire regime. To

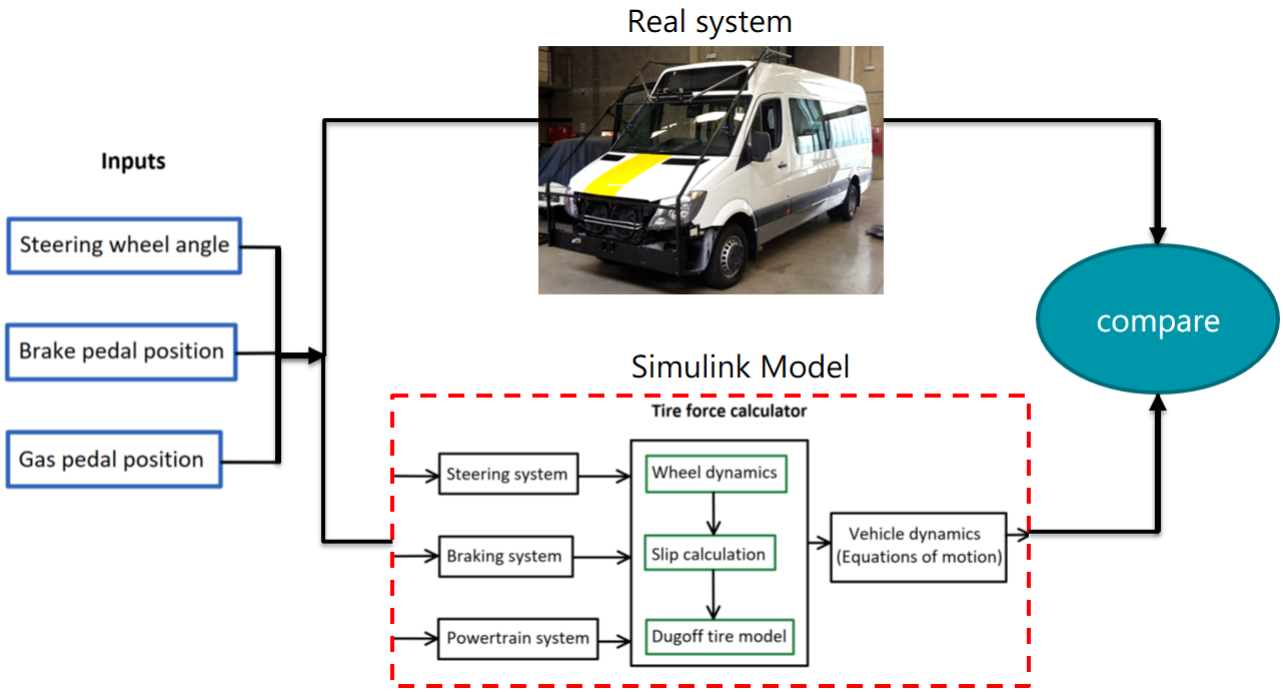

Figure 5.1: Validation overview

reach higher accuracies, however, the constants of the model has to be improved and other effects e.g. camber angle, toe angle have to be considered as well.

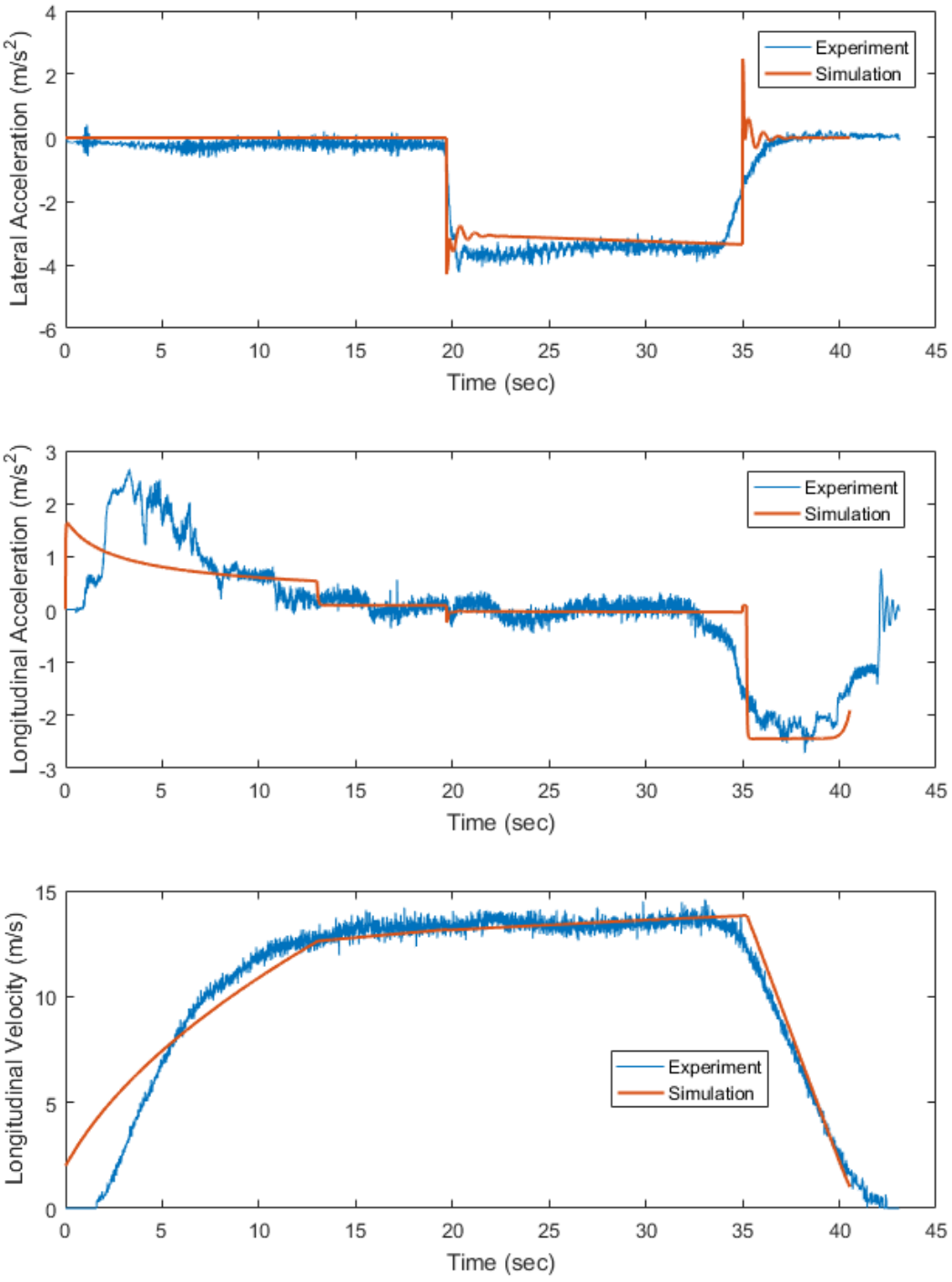

Figure 5.2: Step steer simulation and experiment comparison (Part I)

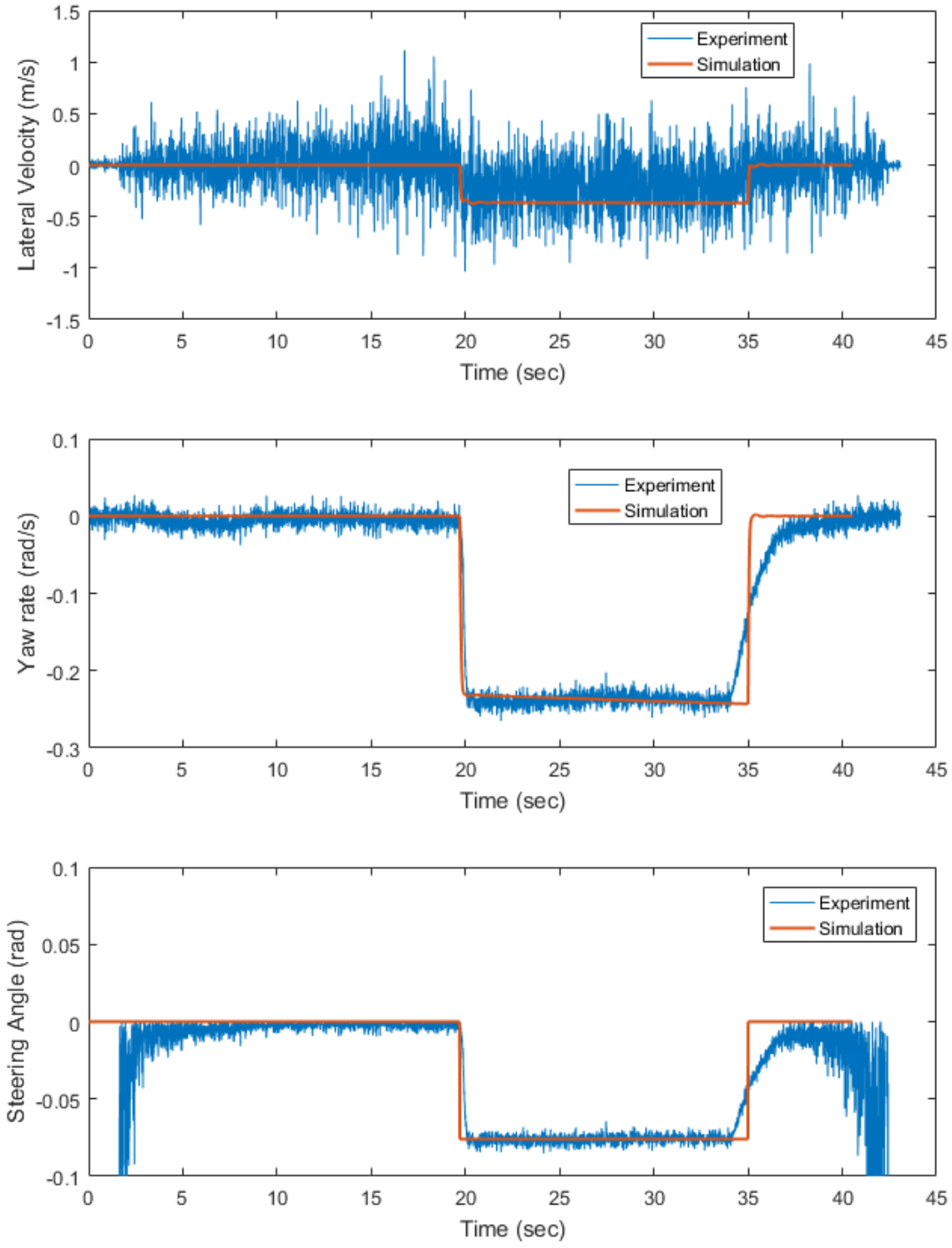

Figure 5.3: Step steer simulation and experiment comparison (Part II)

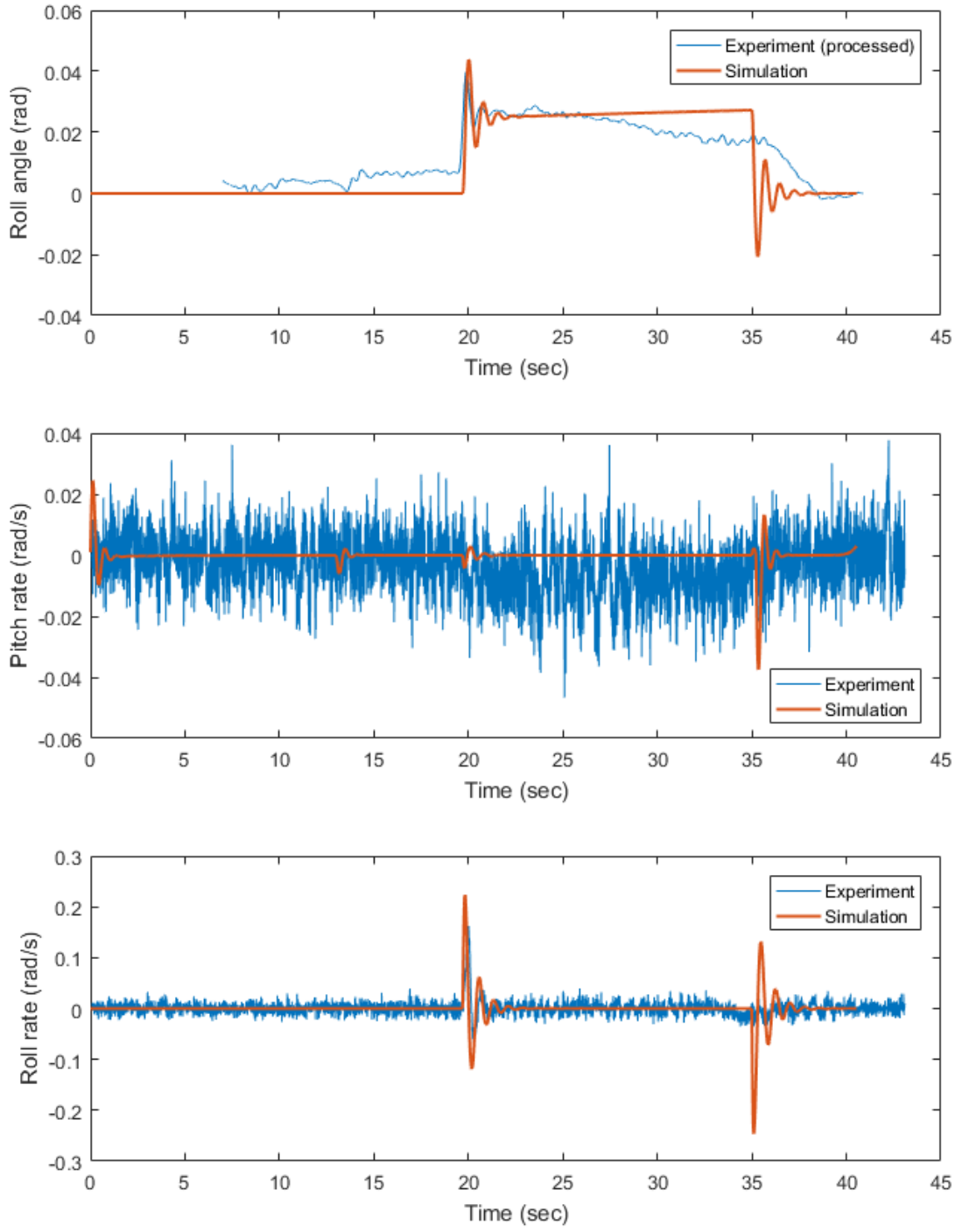

Figure 5.4: Step steer simulation and experiment comparison (Part III)

Chapter 6

Future work

Some tests left unfinished at the end of this study, hence it is strongly recommended to perform these tests and use their results in the model to improve accuracy. Most of the tests need simple equipment and can be done with low cost.

6.1 Center of gravity height

In [14] the center of gravity for other versions of Mercedes Benz Sprinter is given.

$$h_{CG} = 0.84m \tag{6.1}$$

Since the rental company did not reply, it was not feasible to rent a scale and implement the center of gravity height test. Hence the value in 6.1 is used which clearly is not accurate because of the vehicle version diversity. One future work could be obtaining the center of gravity height value by implementing the aforementioned test.

6.2 Rolling road (Dyno test)

There were some technical and non-technical problems that caused the dyno test to be postponed to another time. To obtain more accurate lookup table from wheel torque to gas pedal position, the dyno test result can be extremely useful. The rolling road software is capable of high-accuracy engine torque calculation and having the drive-by-wire installed, one can obtain the look up table to be implemented for both the longitudinal and two track models. It should be noted that the prerequisite test for the dyno (Friction test at LPG) has been done before.

6.3 Brake lookup table

The data needed for this task is already available. Hence, the lookup table can be made as explained in Section 4.2.2 in order to enhance the longitudinal controller.

6.4 CAN access

Some parameters were estimated and not directly measured. Steering angle, gas and brake pedal position can be accessed from the vehicle CAN bus. After which the estimated parameters can be replaced by the new accurate data for each experiment.

6.5 Roll and pitch angle measurement

For some unknown reasons the IMU does not give very accurate results for roll and pitch angle even after calibration. The angles output have offset and too much drift sometimes and even don't match rate of the parameter. So it is recommended to find the cause of this issue and eliminate it for future studies.

6.6 Nonlinear tire regime

Tire modelling is one of the most important part of every vehicle's dynamic response analysis. High side slip angle allows the tire to show its nonlinear response behaviour. Some limitations prevented the limit handling test from implementing. Magic tire formula can be used to fit the obtained test data for better fit.

6.7 Pitch center height

There is no common practice to obtain the pitch center height. One possible solution is to do image processing with different amount of pitch angle. Comparing the images will give an approximation for the pitch center height.
In this study, however, it was assumed that the pitch center height is equal to zero based on the obtained experiment data. It should be mentioned that pitch parameter identification has to be redone in case of finding a new pitch center height.

Table 6.1: Vehicle parameters

Vehicle Parameters		
Parameter	Symbol	Value
Wheelbase	l	4.325 m
Engine power	P_e	95 kW
Vehicle mass	m	3468 kg
Center of gravity distance from front axle	l_f	2.192 m
Center of gravity height	h_{CG}	0.84 m
Roll moment of inertia	I_{xx}	1858 $kg.m^2$
Pitch moment of inertia	I_{yy}	11933 $kg.m^2$
Yaw moment of inertia	I_{zz}	11933 $kg.m^2$
Track-width	t_f	1.708 m
Front roll center height	h'_1	0.4276 m
Rear roll center height	h'_2	0.46 m
Roll stiffness	K_φ	182352 Nm/rad
Roll damping	C_φ	3254 Nms/rad
Pitch stiffness	K_θ	$1.38e+06$ Nm/rad
Pitch damping	C_θ	$80e+03$ Nms/rad
Pitch center height	h''	0 m
Tire radius	r_w	0.35 m
Front axle lateral cornering stiffness	C_1	265500 N/rad
Rear axle lateral cornering stiffness	C_2	279000 N/rad

Bibliography

[1] Bedfordspeedway. http://www.bedfordspeedway.com/toolbox_leaf.htm, consulted on: 10-11-2016. 14

[2] I. Besselink. Vehicle Dynamics 4AT000 lecture notes. 2015. 1, 8, 9, 10, 12, 23, 32, 33

[3] EcoModder. http://ecomodder.com/wiki/index.php/vehicle_coefficient_of_drag_list, consulted on: 26-10-2016. 7

[4] B. Boulkroune N. El Ghouti F. Naets, S. van Aalst and W. Desmet. Design and experimental validation of a stable two stage estimator for automotive sideslip and tire parameters. 2015. 1, 9, 10

[5] J. G. Fernandez. A vehicle dynamics model for driving simulators. 2012. 2

[6] W. R. Garrott and J. P. Chrstos M. W. Monk. Vehicle Inertial Parameters-Measured Values and Approximations. 1988. 13

[7] T. D. Gillespie. Fundamentals of vehicle dynamics. 2006. 13

[8] E. J. Rossetter J. Ryu and J. C. Gerdes. Vehicle sideslip and roll parameter estimation using gps. 2002. 8

[9] St. Germann M. Wrtenberger and R. Isermann. Modelling and parameter estimation of nonlinear vehicle dynamics. 1992. 8

[10] H. B. Pacejka. Tyre and vehicle dynamics. 2006. 2, 12

[11] R. Rajamani. Vehicle dynamics and control. 2006. 19

[12] T. Taniguchi S. Takano, M. Nagai and T. Hatano. Study on a vehicle dynamics model for improving roll stability. 2003. 2

[13] Sprinter Engineering and Compliance Support. Body Builder Information Book. 2007. 20

[14] Upfitter. https://www.upfitterportal.com/en-us/tech-info/model-specification/passenger-van/12, consulted on: 02-12-2016. 43

[15] A. Verkerk. Development and validation of ride handling models for a bmw 318i (e46). 2014. 2

Chapter 7

Appendix

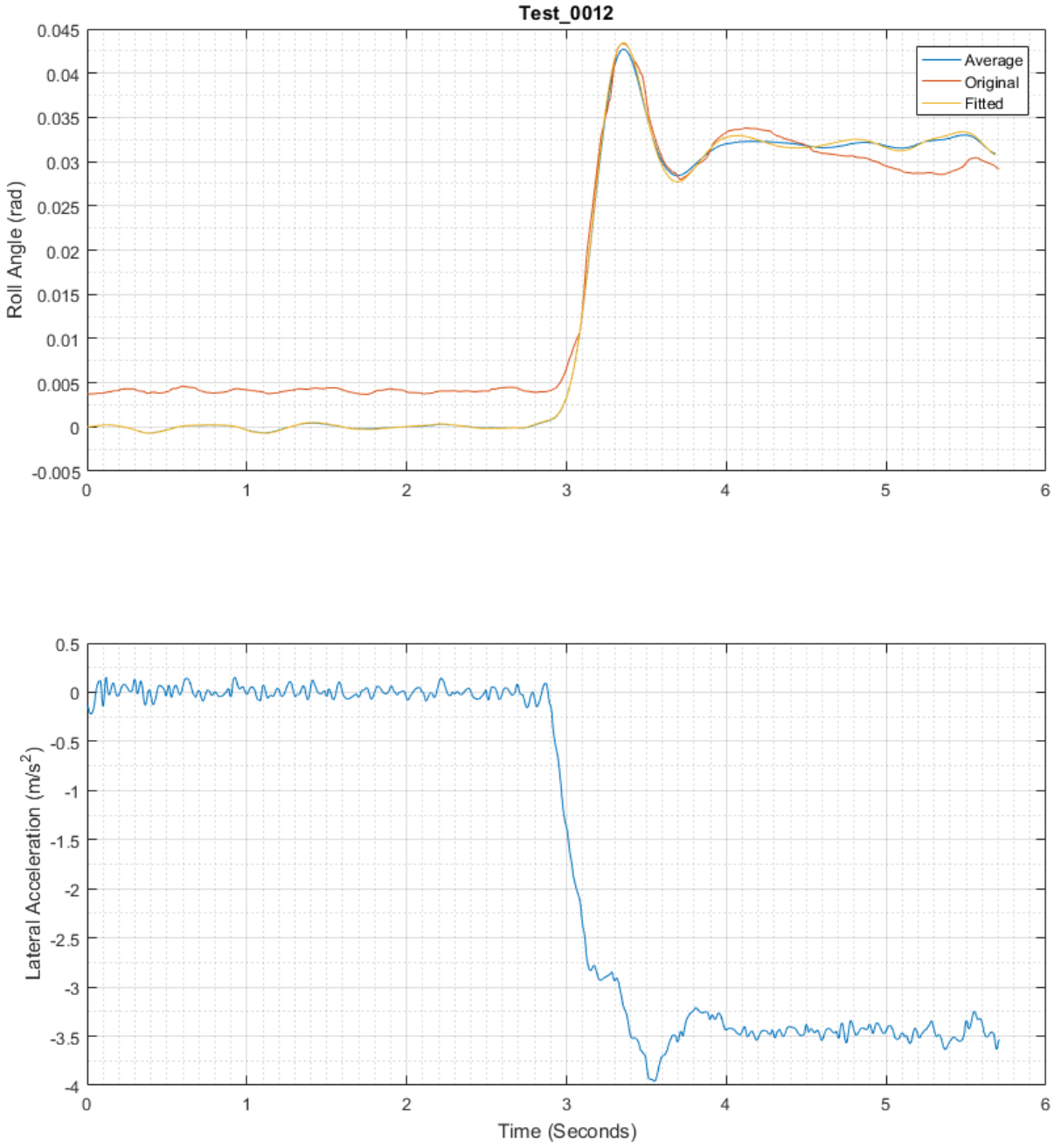

Figure 1: Roll parameter estimation result - Left turn - high speed and high steering input - Original (filtered) measured data together with simulated (fitted) data and the average of all the simulations in adapted SAE sign convention system

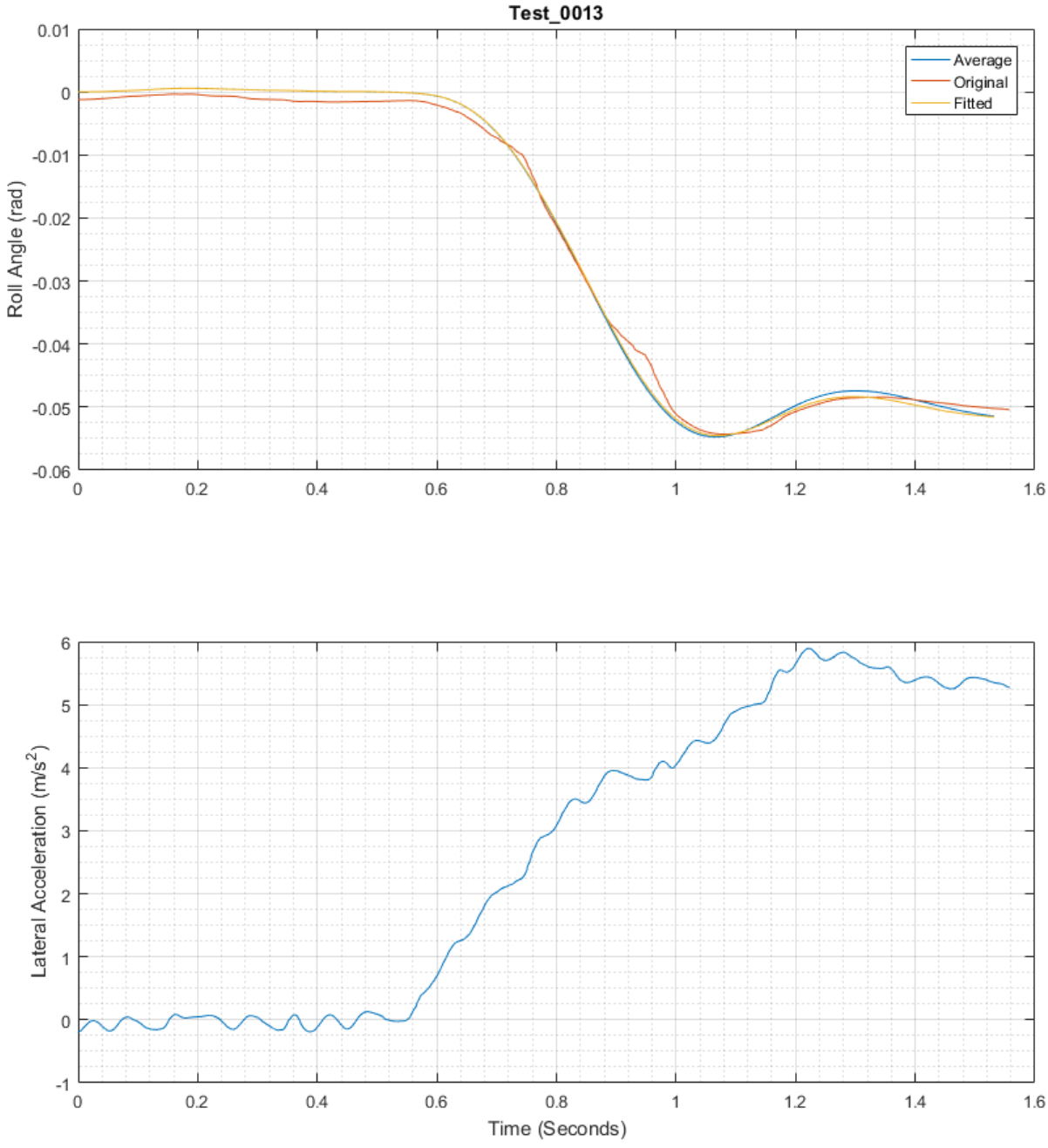

Figure 2: Roll parameter estimation result - right turn - high speed and high steering input - Original (filtered) data together with simulated (fitted) measured data and the average of all the simulations in adapted SAE sign convention system

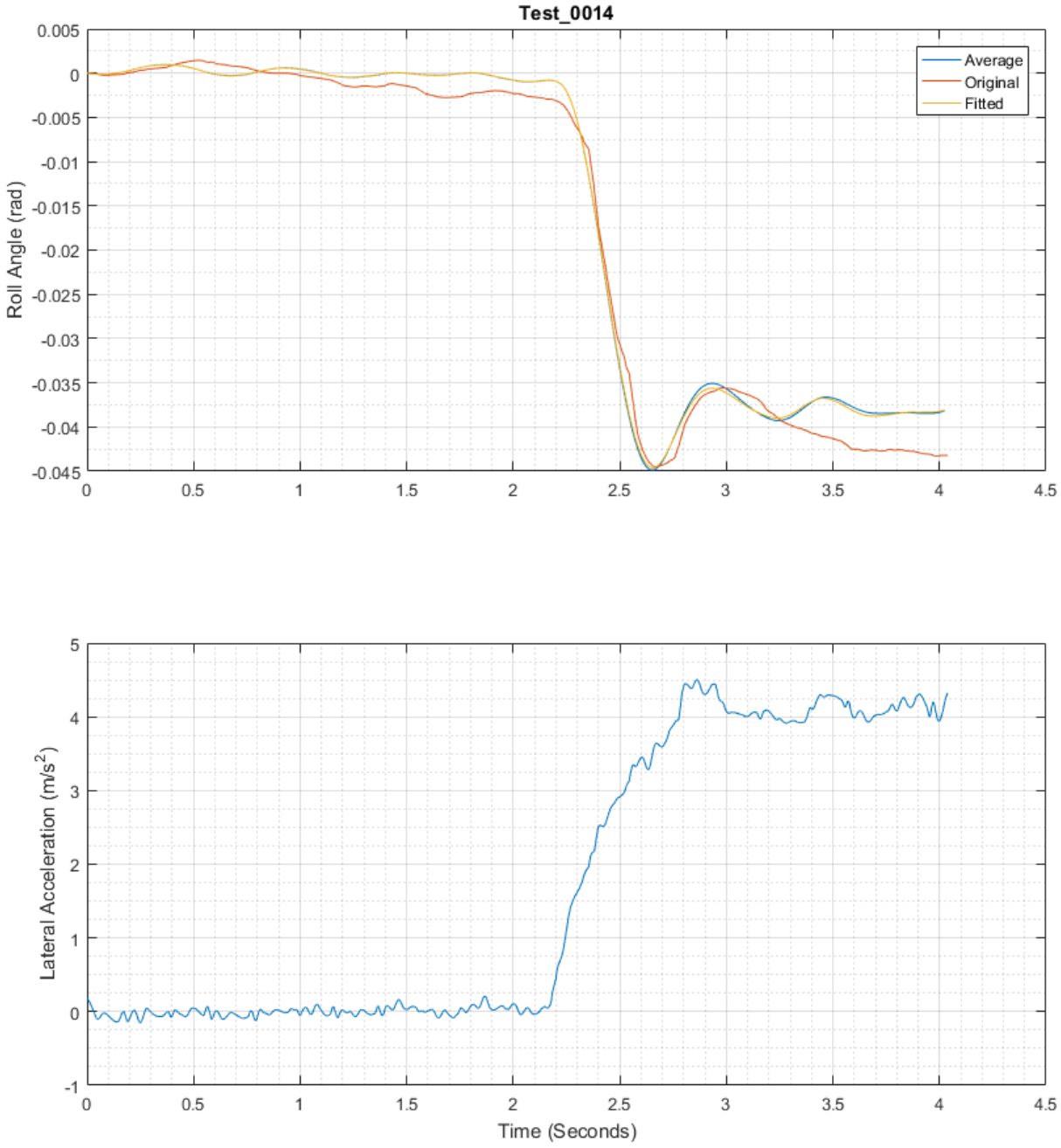

Figure 3: Pitch parameter estimation result - right turn - low speed and low steering input - Original (filtered) data together with simulated (fitted) measured data and the average of all the simulations in adapted SAE sign convention system

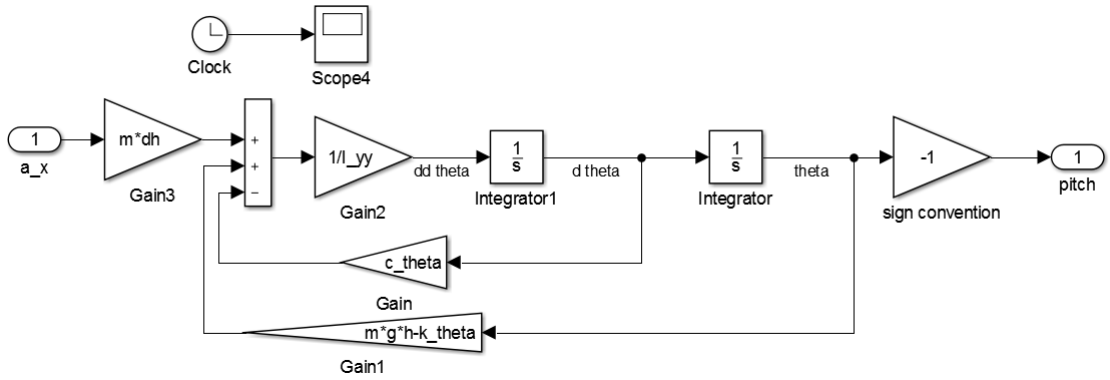

Figure 4: Pitch parameter estimation Simulink model

Engine Torque [N.m]	Gas pedal position [%]				
Actual Engine Speed [RPM]	35	37,5	40	45	50
800	3,094	16,224	40,764	61,799	81,999
900	3,094	16,224	40,764	61,799	81,999
1000	3,094	16,224	40,764	61,799	81,999
1100	3,094	16,223	40,764	61,799	81,999
1200	3,094	15,659	40,764	61,799	81,999
1300	3,094	15,424	40,764	61,799	81,999
1400	3,094	14,675	40,764	61,799	81,999
1500	3,094	12,762	40,764	61,799	81,999
1600	2,317	10,951	39,374	61,799	81,999
1700	3,547	11,713	38,504	59,933	81,999
1800	3,547	14,267	36,714	55,790	81,999
1900	3,547	14,721	36,063	51,972	81,999
2000	3,547	14,721	35,586	49,230	81,999
2100	3,547	14,721	35,746	48,726	80,416
2200	3,547	14,721	36,728	48,599	74,846
2300	3,547	14,721	36,728	49,231	72,442
2400	3,547	14,721	36,728	51,602	70,235
2500	3,547	14,721	36,728	52,958	69,166
2600	3,547	14,721	36,728	52,958	69,037
2700	3,547	14,721	36,728	52,958	69,697

Figure 5: Look up table of engine torque to gas pedal position conversion

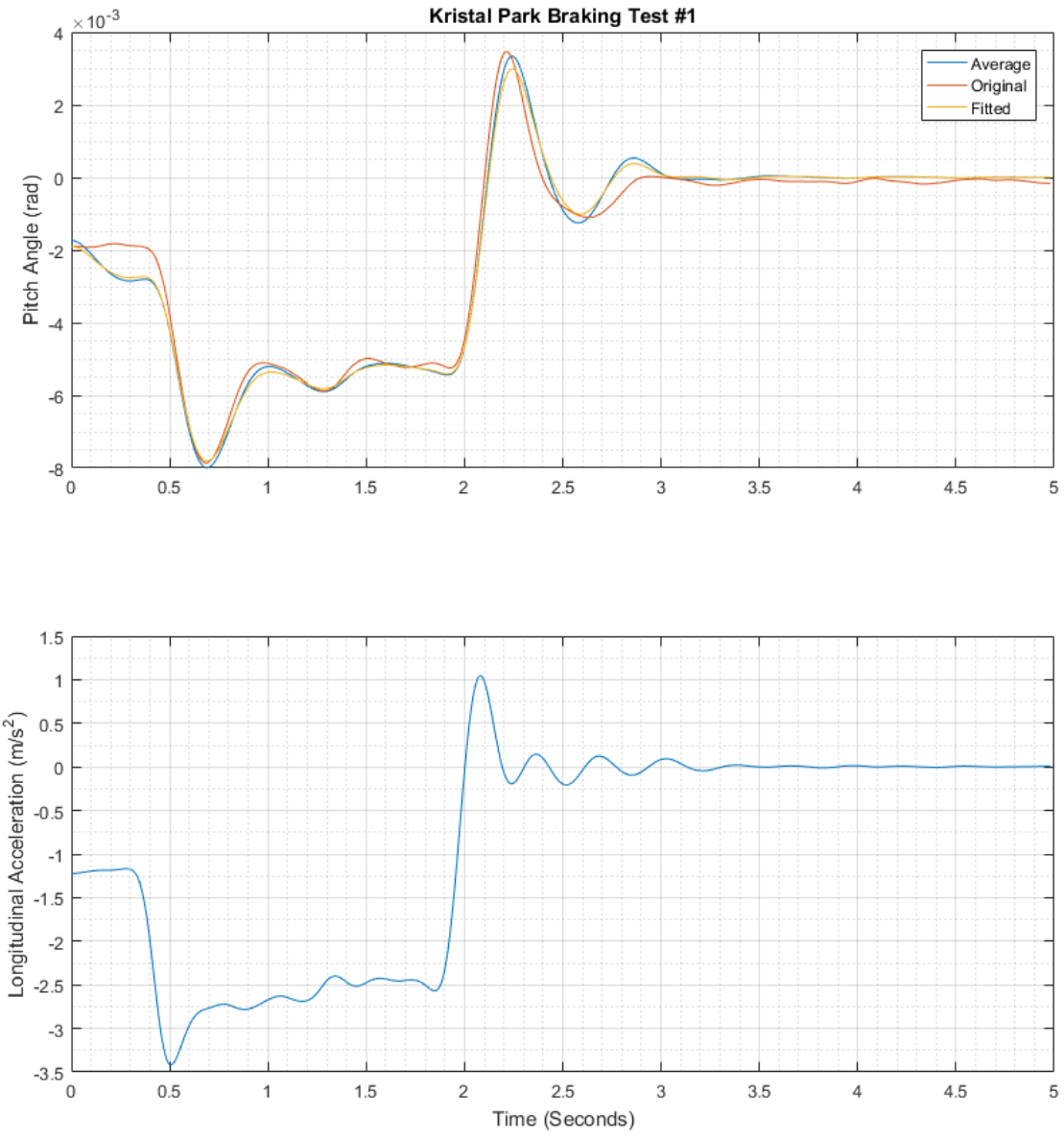

Figure 6: Pitch parameter estimation result for MB Sprinter (1) - Original (filtered) measured data together with simulated (fitted) data and the average of all the simulations in adapted SAE sign convention system

From North to South (In Seconds)	
100 to 90	5
90 to 80	6,93
80 to 70	7,74
70 to 60	9,61
60 to 50	9,4
50 to 40	13,74
40 to 30	13,4
30 to 20	16,94
20 to 10	23,24
10 to 0	37,08

From South to North (In Seconds)	
100 to 90	4,87
90 to 80	6,12
80 to 70	7,95
70 to 60	8,78
60 to 50	11,51
50 to 40	11,15
40 to 30	14,72
30 to 20	17,78
20 to 10	21,72
10 to 0	28,28

	AVG. (in Seconds)	AVG. Deviation from North to South (in %)
100 to 90	4,935	1,32
90 to 80	6,525	6,21
80 to 70	7,845	-1,34
70 to 60	9,195	4,51
60 to 50	10,455	-10,09
50 to 40	12,445	10,41
40 to 30	14,06	-4,69
30 to 20	17,36	-2,42
20 to 10	22,48	3,38
10 to 0	32,68	13,46

Figure 7: Dyno software requirement - free rolling from 100 to 0 kph - rolling friction adaption test result at LPG

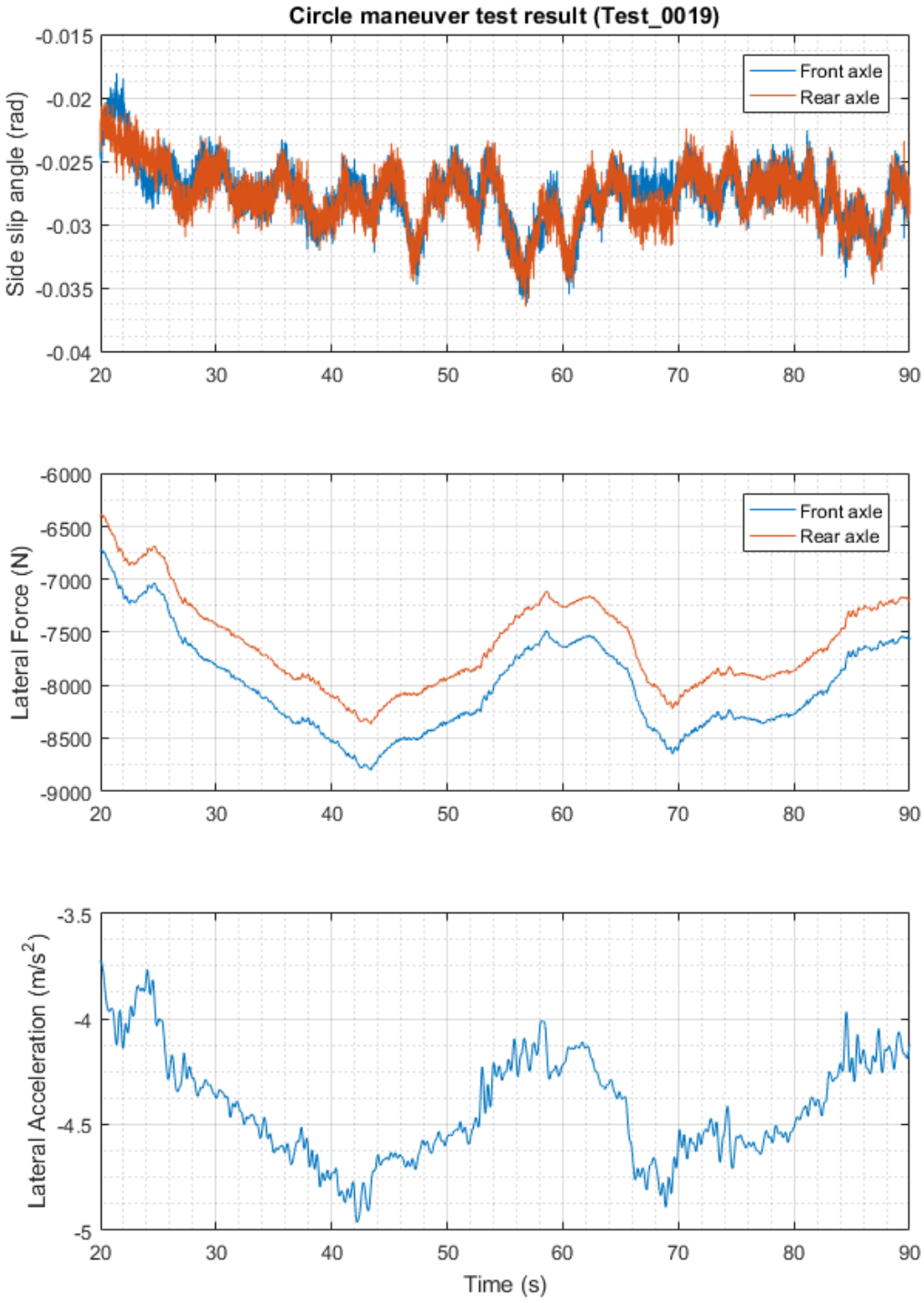

Figure 8: Results for circle maneuver test (Test_0019)